diversity

MDPI

Article

Benthic Community Metrics Track Hydrologically Stressed Mangrove Systems

Amanda W. J. Demopoulos [1,*], Jill R. Bourque [1], Jennifer P. McClain-Counts [1], Nicole Cormier [2] and Ken W. Krauss [3]

[1] U.S. Geological Survey Wetland and Aquatic Research Center, 7920 NW 71st St., Gainesville, FL 32653, USA; jbourque@usgs.gov (J.R.B.); jmcclaincounts@usgs.gov (J.P.M.-C.)
[2] School of Natural Sciences, Macquarie University, Sydney, NSW 2109, Australia; nicole.cormier@hdr.mq.edu.au
[3] U.S. Geological Survey Wetland and Aquatic Research Center, 700 Cajundome Blvd, Lafayette, LA 70506, USA; kraussk@usgs.gov
* Correspondence: ademopoulos@usgs.gov; Tel.: +1-352-264-3490

Abstract: Mangrove restoration efforts have increased in order to help combat their decline globally. While restoration efforts often focus on planting seedlings, underlying chronic issues, including disrupted hydrological regimes, can hinder restoration success. While improving hydrology may be more cost-effective and have higher success rates than planting seedlings alone, hydrological restoration success in this form is poorly understood. Restoration assessments can employ a functional equivalency approach, comparing restoration areas over time with natural, reference forests in order to quantify the relative effectiveness of different restoration approaches. Here, we employ the use of baseline community ecology metrics along with stable isotopes to track changes in the community and trophic structure and enable time estimates for establishing mangrove functional equivalency. We examined a mangrove system impacted by road construction and recently targeted for hydrological restoration within the Rookery Bay National Estuarine Research Reserve, Florida, USA. Samples were collected along a gradient of degradation, from a heavily degraded zone, with mostly dead trees, to a transition zone, with a high number of saplings, to a full canopy zone, with mature trees, and into a reference zone with dense, mature mangrove trees. The transition, full canopy, and reference zones were dominated by annelids, gastropods, isopods, and fiddler crabs. Diversity was lower in the dead zone; these taxa were enriched in ^{13}C relative to those found in all the other zones, indicating a shift in the dominant carbon source from mangrove detritus (reference zone) to algae (dead zone). Community-wide isotope niche metrics also distinguished zones, likely reflecting dominant primary food resources (baseline organic matter) present. Our results suggest that stable isotope niche metrics provide a useful tool for tracking mangrove degradation gradients. These baseline data provide critical information on the ecosystem functioning in mangrove habitats following hydrological restoration.

Keywords: carbon; nitrogen; mangrove restoration; stable isotopes; degradation; niches; functional equivalency

Citation: Demopoulos, A.W.J.; Bourque, J.R.; McClain-Counts, J.P.; Cormier, N.; Krauss, K.W. Benthic Community Metrics Track Hydrologically Stressed Mangrove Systems. *Diversity* **2024**, *16*, 659. https://doi.org/10.3390/d16110659

Academic Editor: Thomas Fickert

Received: 6 September 2024
Revised: 18 October 2024
Accepted: 21 October 2024
Published: 25 October 2024

1. Introduction

Healthy mangrove ecosystems provide a variety of ecological and ecosystem services [1]. Mangroves play a key role in the storage of "blue carbon", sequestration supporting the long-term storage of carbon [2,3], and the mitigation of greenhouse gas emissions [4,5]. However, mangrove ecosystems are continuing to decline worldwide due to a variety of factors [6–8], including land use changes and coastal development, which alter the natural hydrology, leading to mangrove mortality and peat collapse [9]. These continued losses have cascading consequences for the ecology and economy [10], with concomitant impacts on biodiversity, energy flow, and food webs, including the fate of organic carbon [11].

In order to combat this loss, restoration programs have implemented a variety of different approaches, including the direct planting efforts of mangrove propagules over broad scales [12] and restoring the natural hydrology [8,12]; the latter approach ideally improves drainage such that the natural flow conditions return, facilitating the dispersal of propagules and natural plant succession [8,9]. However, mangrove ecosystem recovery can take decades following any type of disturbance or restoration action (e.g., 25+ years following direct restoration, [3]), and the degradation of the habitat persists at least in the short-term following hydrological alterations [5,9,13,14].

Chronically stressed mangroves exhibit distinct symptoms in their above- and belowground attributes [9]. After isolation from natural tidal flow and inundation, changes in salinity and water quality lead to the slow health decline and death in mangrove trees, followed by the collapse of the soil surface. Impacts associated with mangrove degradation and death include changes in the physical structure and biogeochemistry of soils, altering organic matter inputs and porewater dissolved oxygen, which directly affect mangrove-dependent benthic faunal communities [15].

Mangrove benthic fauna have complex life histories and utilize connected habitats [16–18], playing key roles in carbon cycling and organic matter degradation [16,19], and thus serving as key facets of ecosystem functioning and the provisioning of services. These communities are composed of mobile and sessile epifauna (those living on the sediment and/or root surfaces) and infauna (sediment dwellers), typically adapted to extreme environments, including hypersaline and hypoxic conditions, and capable of manipulating the physical and chemical nature of refractory organic matter [20]. For example, brachyuran crabs occupy multiple habitat zones, from arboreal to burrowing forms. Certain species facilitate the decrease in ammonium and sulfide concentrations via bioturbation [16] and increase leaf-litter decomposition, consequently impacting mangrove productivity, and the retention and export of organic matter [20]. Mangrove loss is directly tied to changes in the biodiversity of the food web [21] due to the decline in habitat and modification in the availability of organic matter to the benthos [22]. As mangrove forest structural complexity and biomass increase with maturity, so does the availability of habitat and detrital food sources for new recruits and resident fauna [23]. Likewise, as mangrove forest structure and belowground root biomass decline, leading to open canopy conditions and the reduction in a food bank via leaf litter, benthic communities and their associated trophic ecology will shift in response [11,15,22]. For example, the composition of ocypodid and sesarmid crabs and mollusc taxa, typically epifaunal dominants and ubiquitous across mangrove systems worldwide, have proven useful indicator groups of ecosystem health given that their composition has been demonstrated to shift along mangrove degradation gradients ([15] and references therein). Mangrove infauna in general have proven reliable indicators of habitat and ecosystem change as their relative composition (e.g., the proportion of polychaetes vs. amphipods) provides insights into their sensitivity to disturbance [24,25]. Thus, measuring benthic community characteristics, including composition, diversity, density, and taxa redundancy, can inform the degree of the decline or recovery of their associated habitat [18,26–28].

Examining the trophic ecology of communities provides an additional dimension into the ecosystem functioning of a healthy mangrove [23,29], or disturbed or recovering habitat (cf. [30]). Stable isotope analysis, for example, provides a complementary approach to examining benthic community metrics. Stable isotope analysis has been successfully used to understand mangrove food webs in particular [31], and as a tool to track mangrove ecosystem recovery [15]. The bivariate space occupied by consumer and primary producer isotope values may be used to approximate their overall isotopic niche, which can inform their trophic niche [32,33]. Metrics that approximate this isotopic niche have improved our ability to make comparisons in habitat trophic ecology, including niche location, overlap, niche width, or diversity, both within and among communities over time. By examining bivariate isotopic niche space, one can quantify changes in food-web characteristics due to disturbance or restoration, including the modification of dominant energy pathways or the

overall niche space. For example, Demopoulos et al. [23] postulated that the development of mangrove detritus-based food webs, from algal-dominated to mangrove-dominated, is a function of mangrove forest age, where age-driven shifts in organic matter accumulation and the corresponding isotopic signals have been observed in a variety of detritus-based ecosystems (cf. [34,35]). These changes can be directly measured through the analysis of consumer isotopes and the calculations of community-wide isotope metrics that approximate trophic niche space, diversity, breadth, and redundancy [32]. Thus, isotopic metrics provide a mechanism to track the changes in ecosystem functioning following disturbance or restoration actions.

Clearly, degradation can result from multiple factors and cumulative effects, which play into the overall status of a mangrove environment [36]. The application of intermediate benchmarks and indicator metrics described below to track mangrove ecosystem change and to help estimate the status of recovery could improve the understanding of the timescales for the recovery of full ecosystem functioning. This study examined a stressed and degraded mangrove habitat that was recently subjected to hydrological restoration using a multi-tracer, multidimensional approach described below. We used a space-for-time analysis, examining the mangrove system along a degradation gradient, from dead, transitional, and full canopy zones, and compared these to reference zones that contained mature mangrove forests with similar plant composition. These different mangrove zones represented successional status. We hypothesized that epifaunal and infaunal community composition and structure would differ among zones, and these differences would be driven by gradients in the above- and belowground physical and biogeochemical attributes. Likewise, given the gradient in available primary food resources across habitat zones, we hypothesized that the trophic diversity and overall food webs, inferred using stable carbon and nitrogen isotopes and isotope-derived community-wide metrics, would also be distinct by zone and mangrove maturity, where greater trophic diversity and shifting isotopic baselines is expected with increased mangrove maturity and available primary sources (Figure 1). By combining traditional ecological metrics with stable isotope community analysis, this study provides baseline community ecology information in these environments and identifies key metrics to track over time to help ascertain timescales for recovery or continued ecosystem decline.

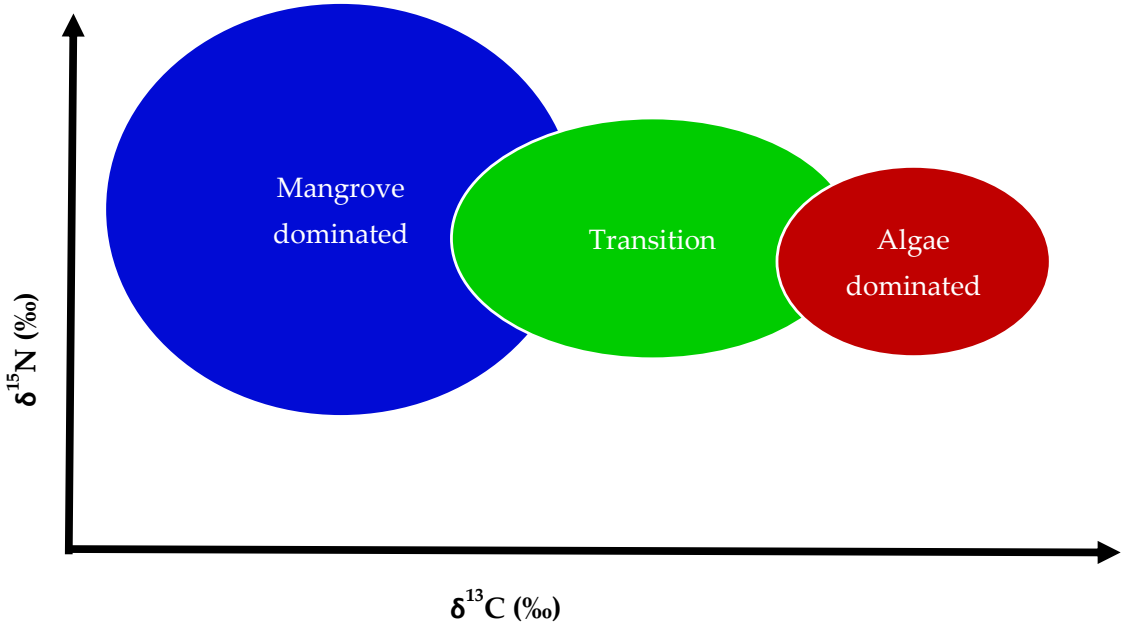

Figure 1. Conceptual diagram of the hypothesized isotopic niche patterns based on the maturation of detrital pathways and increased diversity of available carbon resources.

2. Methods

2.1. Study Site

Rookery Bay National Estuarine Reserve (RBNERR), located on the southwest coast of Florida, USA, protects 44,515 hectares of coastal area and contains approximately 18,553 hectares of mangrove forests. Marco Island is a residential area located within the RBNERR. The development of the island as residential, in particular, the construction of County Road 92 (CR-92), has caused significant long-term stress and mortality to the local mangrove forests [8]. CR-92 restricted tidal flow into the study wetland, fragmenting and damaging the mangrove forest [8,9]. Efforts to restore natural hydrology to this mangrove-forested area to pre-CR-92 conditions began in a 1.6-hectare mangrove die-off area in 2012. Restoration activities included digging several small trenches to enable tidal connection and reestablish tidal flow to the area. While the effort was small in scale, some rehabilitation was evident in the most degraded zones [37] and included sustained tidal flow and the natural recruitment and establishment of native mangrove species.

To assess the effects of hydrological restoration efforts on the biological community, sampling locations were established in the restoration area of RBNERR off CR-92 and on Horrs Island, a peninsula separated from Marco Island by a small tidal creek (Figure 2). Mangrove species present at both sampling locations included *Rhizophora mangle* and *Avicennia germinans*. *Laguncularia racemosa* was also present in the restoration area. Within the restoration area, two sites (T1 and T2) were established across the hydrological stress gradient that encompassed three zones: open canopy (dead), transitional, and full canopy (Figure 2A). The dead zones consisted of mudflats with dead trees and minimal or open canopy cover, whereas the transitional zones were composed of saplings, some live canopy cover, and often the presence of *Batis maritima* (Figure 2C). Lastly, full canopy zones had mature mangrove trees and maximum canopy cover (Figure 2C). Within each zone, replicate 0.25 m^2 quadrats (n = 6, labeled A–F) were established at 5 m intervals along transects running parallel to habitat boundaries, with the corners marked using 0.25″ PVC pipe. An additional site was established (T5) on Horrs Island representing the most proximal and best representation of a natural healthy mangrove habitat (reference zone, Figure 2B). Three replicate transects (labeled A, B, and C) were established with replicate 0.25 m^2 quadrats set up like T1 and T2.

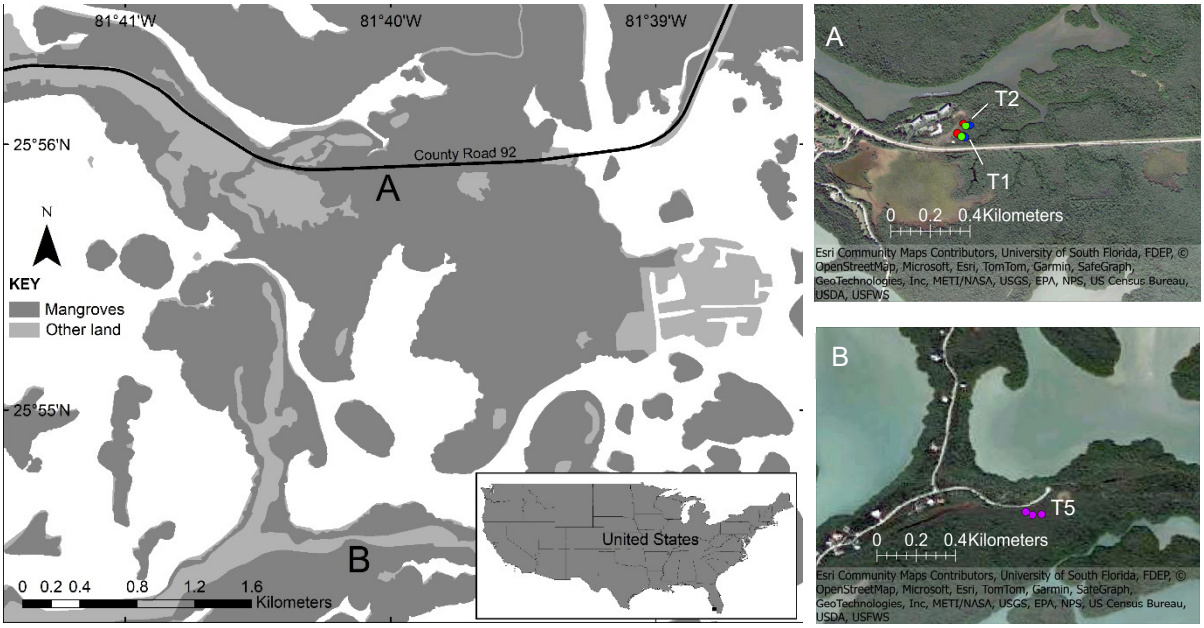

Figure 2. *Cont.*

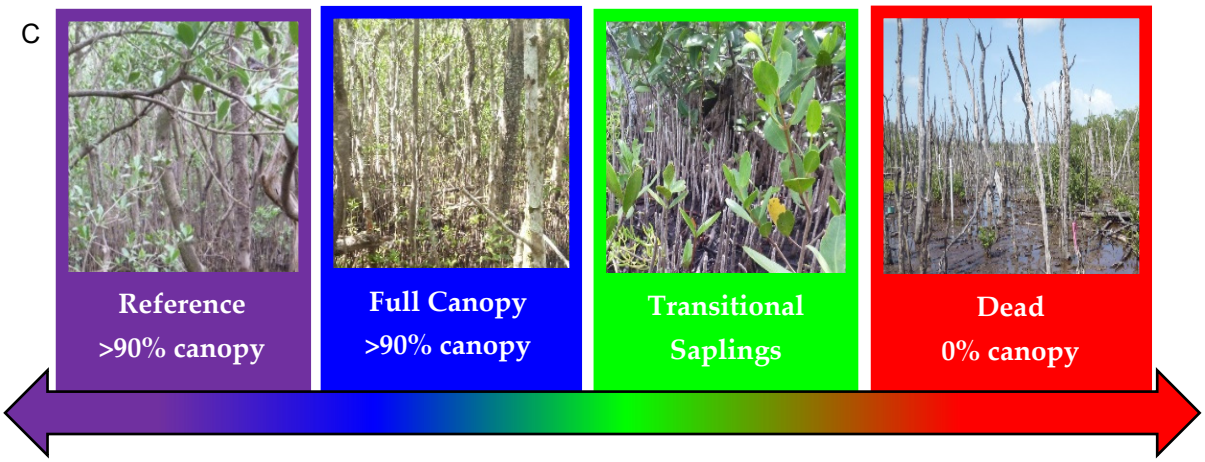

Figure 2. Location of the study area in southwest Florida sampled during winter (January) and summer (August) 2015. (**A**) Two sites (T1 and T2) were established in an area targeted for hydrological restoration on Marco Island, Florida. The points represent three different zones: dead (red), transitional (green), and full canopy (blue), sampled along each transect in the restoration area. (**B**) Additional transects were established within a natural mangrove habitat (T5) on Horrs Island. The purple points represent the locations of three reference transects in mature mangroves. (**C**) Representative habitats in each zone sampled during this study.

2.2. Field Sampling

The sampling occurred in the early morning during daylight hours both in winter (January) and summer (August) in 2015; these events corresponded to a mixture of tidal cycles. The quantitative observations of flora and epifauna presence were recorded within the six quadrats at each zone for the three sites (T1, T2, and T5; Figure 2) at both time points. Flora counts included densities (# m^{-2}) of mangrove prop roots, pneumatophores, seedlings, saplings, trees, and/or other plant or algae taxa (e.g., *Batis* sp. and macroalgae) present within a quadrat. Specific epifauna, including crabs, snails, bivalves, insects, fish, or biogenic features (e.g., burrows or insect tubes) were also recorded. For the other sampling parameters (light, redox potential, porewater, sediment cores, and BMA), sampling and measurements were conducted at every other quadrat (January 2015 = quadrats ACE; August 2015 = quadrats BDF) along each zone. Alternating sampled quadrats for each time point (ACE then BDF) reduced the potential disturbance impacts associated with repeated sampling at the same location. Light at the sediment surface was measured using an Apogee QMSS-S quantum meter. Porewater salinity measurements within the upper 2 cm of sediment were recorded using a handheld refractometer. Redox probes were inserted into the sediments at 5, 15, and 30 cm depths to examine redox potential, enabling comparisons to previous studies (e.g., [38]) and capturing the uppermost sediment layers where infauna reside. Porewater was extracted in situ using a 50 mL syringe attached to a sipper tube [38] inserted to 5, 15, or 30 cm depth. YSI probes were inserted into the extracted porewater to record salinity (YSI model 30), temperature (°C), dissolved oxygen (mg/L), percent oxygen, and conductivity (mS) (YSI model 550A) for each porewater sample. Three sediment cores (6.35 cm diameter) were inserted approximately 2 cm into the ground outside of the quadrats (within 10 cm) for (1) infauna for stable isotope analysis (SIA) (referred to as "infaunal cores" from hereon), (2) infauna community assemblages ("macrofauna cores") and belowground plant organic biomass, and (3) sediment organic carbon, total nitrogen, stable carbon and nitrogen isotopes, and grain size ("sediment chemistry cores"). The infaunal cores were placed in 250 mL jars topped off with filtered seawater and stored in the refrigerator until they were sieved and sorted live for SIA. The macrofauna cores were placed in 250 mL jars and preserved in a 10% formalin–seawater solution for later sorting. The sediment chemistry cores were placed in a whirlpak and homogenized, and approximately 2 mL of material was placed in a vial for SIA, and then

frozen at −20 °C. For the collection of benthic microalgae (BMA), a 10 mL syringe with the tip removed was inserted into the sediment to extract ~10 mL of surface sediment. BMA sediment was placed in a 15 mL cryovial and frozen at −20 °C until laboratory extractions for SIA. (see details below). Flora (mangrove leaves, detritus, *Batis* sp., and algae) and epifauna were also collected, targeting 5–10 specimens per zone within the three transects, and frozen for SIA. Samples of standing water were collected along the north side of CR-92 and subsequently filtered through a pre-combusted 47 mm GFF filter to isolate particulate organic material (POM).

2.3. Isotope Analyses

BMA were extracted from sediments using the Ludox extraction technique as described in Moseman et al. [39]. Briefly, equal volumes of homogenized surface sediment and deionized water were added to a 15 mL centrifuge tube, vortexed, and then centrifuged, and the resulting supernatant was discarded. Ludox was then added to the centrifuge tube, the contents were vortexed again, and then centrifuged. The resulting golden-brown layer of microalgae was extracted using a pipette and transferred to a pre-combusted GFF filter. The filters were examined under the dissecting scope to remove detritus and fauna.

The infauna cores were first sieved over stacked 1 mm and 300 µm meshes and then sorted live in seawater for dominant macrofauna (>300 µm). The sorted infauna were dipped in deionized water, placed in preweighed tin capsules, and then dried and reweighed to determine sample weight. In the laboratory, flora and epifauna samples were identified and dissected. For consistency, tissue was removed from similar body regions based on taxa [40]. The tissues were dried to a constant weight at 50–60 °C, ground to a fine powder with mortar and pestle, and weighed into tin capsules for SIA. Invertebrates (both epi- and infauna) were acidified with 10% platinum chloride mixed with 1 N hydrochloric acid to remove inorganic carbon, then dried. The POM filters were dried and weighed. The POM and BMA filters were then acidified with 1 N hydrochloric acid, dried (50–60 °C), and scraped into tin capsules for SIA. The sediments subsampled from the sediment chemistry core were dried (50–60 °C), then homogenized, and sent to Washington State University (WSU) for acidification with 1 N phosphoric acid prior to encapsulating in tin capsules for SIA.

The SIA samples were analyzed for stable carbon and nitrogen composition referenced to Vienna PeeDee Belemnite and atmospheric nitrogen gas, respectively, at WSU using a Costech (Valencia, Santa Clarita, CA, USA) elemental analyzer interfaced with a GV instruments (Manchester, UK) Isoprime isotope ratio mass spectrometer. Precision was verified using egg albumin calibrated against the National Institute of Standards reference materials and reproducibility was monitored using organic reference standards [40] and duplicate samples. Isotope ratios were expressed in standard delta notation, $\delta^{13}C$ and $\delta^{15}N$, in per mil (‰). The long-term standard deviation for samples versus standards is 0.3‰ for $\delta^{13}C$ and 0.5‰ for $\delta^{15}N$.

2.4. Sediment Analyses

The macrofauna cores were sieved over stacked 1 mm and 300 µm meshed sieves. The sieved sediments were sorted under a dissecting microscope, and macrofauna were identified to family level or higher and stored in 80% ethanol. The identified infauna from both the 1 mm and 300 µm fractions were combined for analyses. Organic material was separated from the residual material from the macrofauna core fractions, including the dense root matter in the 1 mm fraction and the finer organic particles via flotation in the 300 µm fraction, and dried to a constant weight at 50–60 °C to estimate the belowground organic biomass. The sediment chemistry cores collected for grain size analysis were sieved over a 2 mm mesh to remove root matter, and hydrogen peroxide was added to remove the remaining organic matter. The sediments were then sieved over a 63 µm mesh to separate the mud (<63 µm) and sand (>63 µm) fractions and dried to a constant weight at 110 °C.

2.5. Statistical Analysis

The raw data of macrofauna, epifauna, sediment and porewater chemistry, and stable isotope content can be found in the associated data release [41]. Two-way analysis of variance (ANOVA) tests indicated no difference between the sites T1 and T2, allowing data to be pooled for all the statistical analyses presented in the results below (Supplemental Table S1). Univariate metrics, including the densities of individuals, biodiversity, stable isotopes, and environmental parameters were analyzed using the program R [42]. One- and two-way ANOVAs were used to test for differences between the sampling periods (winter and summer) and among zones (dead, transition, full canopy, and reference) followed by Tukey's HSD for multiple comparisons. All the data were tested for normality and homoscedasticity using Shapiro–Wilk and Levene's test [43] and $\log_e$-transformed when necessary. If transformation did not achieve normality or homoscedasticity, a non-parametric Kruskal–Wallis test was used followed by a pairwise Wilcox test with a Holm correction for multiple comparisons. A significance level of $p < 0.05$ was used in all the tests. Five samples were excluded from the analyses of sediment stable isotopes (S1T-C Winter, S1D-E Winter, S5B-D Summer, S5C-D Summer, and S5C-F Summer) due to $\delta^{13}C$ and $\delta^{15}N$ values outside the 99% confidence intervals of the samples.

The epifaunal community structure was assessed by examining the overall contribution (densities) of *Minuca* sp., Mytilidae, Cerithiidae, *Melampus coffea*, fish, Insecta, insect tubes, and burrows. The infaunal community structure was assessed by quantifying the contribution of higher-level taxa: Polychaeta, Oligochaeta, Mollusca, Insecta, Turbellaria, and other taxa. Other taxa included Decapoda, Anthozoa, Hydrozoa, Nemertea, Acari, and Arachnida. The colonial taxa Bryozoa were not included in the density, diversity, and community analyses but were included in the overall taxa numbers. The metrics for biodiversity included the total number of taxa present (Sp), Shannon diversity ($H'\log_e$), and Pielou's evenness (J') based on untransformed family-level or higher-density data in PRIMER version 7. Statistical analyses were not performed on epifauna evenness (J') due to the absence of epifauna in many quadrats resulting in an inability to calculate the metric. The multivariate analysis of the epifaunal and infaunal communities was performed on square root-transformed family-level or higher-density data using Bray–Curtis similarities in PRIMER 7 [44]. Differences in the epifaunal and infaunal communities with respect to zone and sampling time period were examined using the analysis of similarities (ANOSIM) and visualized with non-metric multidimensional scaling (nMDS). Similarity of percentages (SIMPER) was used to identify the taxa responsible for discriminating between zones and sampling periods and to assess the variability of the communities within those groups. Cluster analysis (CLUSTER) combined with similarity profile analysis (SIMPROF) was additionally used to determine similarity groupings. The samples containing no epifauna ($n = 25$) were excluded from the epifaunal community analyses. The corresponding samples in the epifauna similarity matrix were compared to the infauna similarity matrix using the RELATE function to assess the correlation between the epifaunal and infaunal communities.

Several environmental and biological drivers of community structure and composition were also examined and incorporated into a model. The environmental drivers included sediment and porewater characteristics: percent sand content, percent carbon and nitrogen content, $\delta^{13}C$ and $\delta^{15}N$, redox potential, light, surface salinity, porewater oxygen concentration, percent oxygen content, salinity, temperature, and conductivity. The biological drivers included belowground plant biomass, and densities of epifauna (Cerithiidae and insect tubes), pneumatophores, seedlings, and trees quantified from the quadrats. Distance-based linear modeling (DistLM) was used to assess the relationship between these potential drivers and the infaunal communities using the PERMANOVA+ add-on package in PRIMER 7 [45]. DistLM performs nominal tests of each variable's explanatory power on community structure and builds a multivariate statistical model of the explanatory power of a suite of variables when considered together to determine the "best" model based on the Akaike information criterion for small sample sizes (AICc). For epifaunal communities, DistLM was performed using the same drivers as included for the infauna,

except for Cerithiidae and insect tubes, since they were already represented in the epifaunal community attributes.

In order to estimate the isotopic niche size and overlap, sample size-corrected standard ellipse area (SEA_c), the Bayesian SEA (SEA_b), and SEA_b overlap were calculated using SIBER packages [33,46] in R version 4.1.3 for the epi- and infauna isotope data from different zones within T1, T2, and T5. While large bivalves had both muscle and gill tissue analyzed, only muscle tissue was included in the statistical analyses because muscle was analyzed consistently across multiple taxa. For SIBER analyses, the "community" category was defined as the sampling period (winter and summer), while the zones were classified under the "group" category (dead, transition, full canopy, and reference). SEA_c was calculated because small sample sizes can lead to bias and result in the underestimation of the population SEA, confounding comparisons between studies that have unequal sample sizes. SEA_b was calculated from 10^4 posterior iterations of SEA_b based on the data set, with mean and 95% credible intervals reported. SEA_b illustrates the total amount of niche space occupied by the "group" (i.e., zone) and can approximate the extent of the trophic diversity and utilized resources. SEA overlap for the different habitats was calculated and expressed as a proportion of the sum of the non-overlapping areas in the ellipses. The calculated values range from 0 to 1, reported here as 0–100% overlap, respectively [33]. The isotopic niche was further evaluated in R using Layman metrics [32,33]. The carbon (CR) and nitrogen (NR) ranges indicate differences between the minimum and maximum values and infer the basal carbon sources and variability in primary production (CR), as well as nitrogen sources and trophic length (NR). The mean distance to the centroid (CD) and mean nearest neighbor distance (MNND) provide information on the trophic diversity and degree of species packing, while the standard deviation of nearest neighbor (SDNND) provides an indicator of trophic evenness. Posterior distribution differences were calculated for SEA_b, CR, NR, CD, MNND, and SDNND to determine statistical significance.

3. Results

3.1. Environmental Characteristics

Several environmental parameters (15 of 18) were significantly different either among zones or time points (Table 1). In general, the dead zone had the highest light levels, higher sediment $\delta^{13}C$ values and mud content, but lower C:N, belowground root biomass, and redox at 15 cm depth (Table 1). Temporal differences were most apparent in the porewater characteristics, with lower temperature, salinity, and conductivity at 30 cm sediment depth occurring in winter, and higher oxygen concentrations and surface salinity in the winter than in the summer. The light levels and sand content were also lower in the winter than in the summer, while the mud content was higher in the winter. Within each zone, the $\delta^{13}C$ and $\delta^{15}N$ values of the surface sediments were consistent (Supplemental Table S2). However, there were among-zone distinctions; the dead zone surface sediments had significantly higher $\delta^{13}C$ and $\delta^{15}N$ values compared to all the other zones. The surface sediment $\delta^{13}C$ values from the transitional zone were higher than full canopy and reference zones (Supplemental Table S2). For the sediment $\delta^{15}N$ values, there was variation between the two time points; while there was no difference in the sediment $\delta^{15}N$ values among transitional, full canopy, and reference for winter, transitional and full canopy both had higher values than the reference in summer.

Table 1. Mean ± SE values for environmental variables within each zone and sampling period. For statistical comparisons: W = winter; S = summer; R = reference; F = full canopy; T = transitional; D = dead; using $\alpha < 0.05$ for the level of significance. Surface porewater salinity (psu) was measured via a refractometer, while a YSI was used for measuring salinity (psu), temperature (T, °C), %O, O_2 (mg/L), and conductivity (Cond, mS) at 30 cm sediment depth. Light (μmol m^{-2} s^{-1} 400–700 nm) was measured at the sediment surface. Roots refers to root biomass and Redox refers to reduction–oxidation potential. Note that different sample sizes were used for isotope and organic content for the winter transitional and dead zones (n = 5), and summer reference zone (n = 6).

Season			**Winter**				**Summer**		**Statistical**
Zone	**R**	**F**	**T**	**D**	**R**	**F**	**T**	**D**	**Comparisons**
Sample Size	9	6	6	6	9	6	6	6	
$\delta^{13}C$ (‰) *	−27.1 ± 0.4	−27.0 ± 0.4	−26.2 ± 0.4	−24.2 ± 0.9	−27.1 ± 0.3	−27.1 ± 0.4	−26.5 ± 0.2	−24.1 ± 0.8	D > T > F = R
%C	22.4 ± 5.2	16.3 ± 1.1	17.5 ± 1.2	19.8 ± 3.0	23.0 ± 4.6	21.9 ± 2.4	16.6 ± 1.9	17.0 ± 1.9	-
$\delta^{15}N$ (‰) ‡*^	2.1 ± 0.6	2.7 ± 0.3	2.2 ± 0.4	4.2 ± 0.6	2.0 ± 0.3	2.8 ± 0.6	3.3 ± 0.2	4.2 ± 0.2	ST > WT, W: D > T = F = R, S: D > T = F > R
%N	1.7 ± 0.4	1.0 ± 0.0	1.1 ± 0.1	1.9 ± 0.3	1.5 ± 0.2	1.3 ± 0.2	1.5 ± 0.2	1.8 ± 0.1	-
C:N *	16.2 ± 2.3	19.7 ± 2.9	18.4 ± 1.3	12.0 ± 1.2	18.1 ± 4.9	21.6 ± 6.2	13.7 ± 2.8	11.1 ± 1.7	F > R = T > D
Light ‡*	58.0 ± 13.7	18.3 ± 1.7	107.2 ± 51.4	1159.3 ± 179.3	613.4 ± 275.6	521.7 ± 230.7	547.2 ± 306.1	1475.8 ± 122.4	S > W, W: D > R = F = T
Grain size									
Sand (%) ‡*	21.86 ± 0.63	33.60 ± 2.92	44.74 ± 7.22	20.01 ± 1.39	30.98 ± 2.39	35.96 ± 1.84	63.14 ± 7.42	36.30 ± 6.45	S > W, W: T = F > R = D, S: T > R = F
Mud (%) ‡*	78.14 ± 0.63	66.40 ± 2.92	55.26 ± 7.22	79.99 ± 1.39	69.02 ± 2.39	64.04 ± 1.84	36.86 ± 7.42	63.70 ± 6.45	W > S, W: D = R > T = F, S: R = F > T
Roots (g) *	4.06 ± 0.60	5.16 ± 0.54	5.62 ± 0.70	2.44 ± 0.69	4.59 ± 0.53	5.49 ± 0.60	4.12 ± 0.35	0.87 ± 0.26	R = F = T > D
Porewater Salinity									
Surface ‡*	49.44 ± 0.82	47.67 ± 1.58	51.17 ± 1.42	48.00 ± 1.06	38.44 ± 1.31	34.67 ± 0.33	40.83 ± 2.85	34.67 ± 0.92	W > S, No zone difference
30 cm ‡*	52.04 ± 0.75	45.55 ± 5.17	57.63 ± 0.84	53.32 ± 2.72	56.59 ± 0.23	51.05 ± 1.15	59.27 ± 1.34	54.47 ± 1.32	S > W, R = T = D > F
T (°C) ‡*	18.79 ± 0.46	21.42 ± 0.22	22.73 ± 0.13	22.00 ± 0.80	29.71 ± 0.34	30.83 ± 0.69	31.52 ± 0.48	30.83 ± 0.49	S > W, W: D = T = F > R,
$\%O_2$ ‡*^	82.62 ± 13.89	67.45 ± 9.03	73.87 ± 9.06	29.72 ± 7.17	20.36 ± 0.76	33.38 ± 1.02	19.40 ± 1.03	47.75 ± 29.25	W > S, W: R > D
O_2 ‡	5.67 ± 0.96	5.13 ± 0.77	12.17 ± 7.11	7.74 ± 5.68	1.55 ± 0.08	2.49 ± 0.07	1.46 ± 0.09	1.38 ± 0.04	W > S
Cond ‡*	75.42 ± 0.72	73.32 ± 1.88	81.95 ± 1.04	76.70 ± 3.47	88.42 ± 0.70	81.67 ± 1.85	94.72 ± 1.21	86.65 ± 1.70	S > W, W: T > F, S: T > D = T > F
Redox (mV)									
5 cm	40.12 ± 60.39	124.80 ± 63.96	78.30 ± 91.61	−120.18 ± 32.81	−67.94 ± 47.64	−67.52 ± 68.03	57.53 ± 68.48	−43.20 ± 32.42	-
15 cm *	−71.34 ± 20.64	69.62 ± 77.89	−3.32 ± 38.66	−127.90 ± 23.76	−82.47 ± 49.25	−45.73 ± 82.84	−57.78 ± 56.27	−147.27 ± 34.27	F > D
30 cm *	−126.49 ± 30.56	−87.03 ± 55.11	−159.25 ± 27.42	−158.00 ± 15.40	−70.34 ± 36.93	−84.88 ± 60.95	−191.85 ± 34.51	−178.20 ± 24.73	No pairwise

‡—indicates significant temporal differences; *—indicates significant differences among zones; ^—indicates significant interaction between zone and time.

3.2. Faunal Diversity and Community Structure

3.2.1. Epifauna

The epifaunal communities differed among the zones and time points (Figure 3; Table 2; Supplemental Tables S2 and S3). The epifaunal density did not differ between time points for all the zones except for dead (Figure 3; Table 2). Among the zones, the densities in the reference zones were the lowest in both seasons, and comparable to the dead zones in the winter (Supplemental Table S4). Shannon diversity (H'log$_e$) followed a similar pattern as density in both seasons, with the lowest diversity occurring in the reference zones (Table 2), while qualitatively, evenness (J') was similar or not detected among all the seasons and zones. Community composition in the reference, full canopy, and transitional zones was dominated by *M. coffea* molluscs which were absent from the dead zone (Figure 3). Additionally, the transitional and full canopy communities were characterized by similar proportions of burrows. Mytilidae molluscs (*Geukensia granosissima*) were only found in the full canopy zones. In contrast, the reference zone community was composed entirely of *M. coffea* and fish. Fish were also observed in the dead zone in winter, indicative of the presence of standing water in these areas. There were temporal differences in the dead and full canopy epifaunal communities but not in the transitional or reference zones (Supplemental Table S2). Cluster analysis identified six distinct community clusters (Figure 4A). The winter reference communities all grouped together, while the summer reference communities, which contained few taxa, grouped with the dead zones, likely due to the presence of few taxa overall. The majority of the full canopy communities grouped together with a subset of the transitional communities, while a few of the transitional communities grouped with the summer dead communities at the lowest percent similarity (43%).

Table 2. Epifaunal and infaunal community metrics, and total flora density collected during winter (January) and summer (August) in 2015. Density (ind. m^{-2}), evenness (J'), and Shannon diversity (H'log$_e$) are presented as mean ± SE values.

Season	**Winter**				**Summer**			
Zone	**Reference**	**Full Canopy**	**Transitional**	**Dead**	**Reference**	**Full Canopy**	**Transitional**	**Dead**
Epifauna								
Sample Size	18	12	12	12	18	12	12	12
Density	3.1 ± 1.1	110.3 ± 10.6	38.3 ± 11.8	4.3 ± 0.8	1.8 ± 0.7	109.3 ± 22.6	48.7 ± 15.9	104.0 ± 16.3
Number of Taxa	1	5	4	3	2	4	4	5
Evenness (J')	-	0.72 ± 0.05	0.73 ±0.08	0.92	0.92	0.61 ± 0.04	0.67 ± 0.13	0.48 ± 0.07
Shannon Diversity (H'log$_e$)	0.0 ± 0.0	0.66 ± 0.07	0.45 ± 0.10	0.05 ± 0.05	0.04 ± 0.04	0.50 ± 0.08	0.26 ± 0.10	0.26 ± 0.08
MVDISP	1.37	0.509	1.031	0.707	0.975	0.862	1.125	0.637
Infauna								
Sample Size	9	6	6	6	9	6	6	6
Density	20,713 ± 3196	12,164 ± 2498	18,589 ± 4201	155,187 ± 19,658	14,955 ± 3804	20,326 ± 4838	19,747 ± 4667	18,273 ± 4574
Number of Taxa	12	15	14	13	9	22	12	10
Evenness (J')	0.62 ± 0.04	0.76 ± 0.03	0.74 ± 0.04	0.39 ± 0.03	0.61 ± 0.07	0.68 ± 0.07	0.74 ± 0.01	0.64 ± 0.06
Shannon Diversity (H'loge)	1.08 ± 0.07	1.55 ± 0.09	1.33 ± 0.05	0.74 ± 0.07	0.81 ± 0.11	1.38 ± 0.18	1.36 ± 0.08	1.10 ± 0.13
MVDISP	0.686	1.265	1.294	0.578	0.995	1.695	0.668	1.266
Flora								
Density	403.8 ± 15.9	550.3 ± 51.8	541.0 ± 31.6	2.3	418.4	425.3	478.0 ± 80.1	47.3 ± 45.2

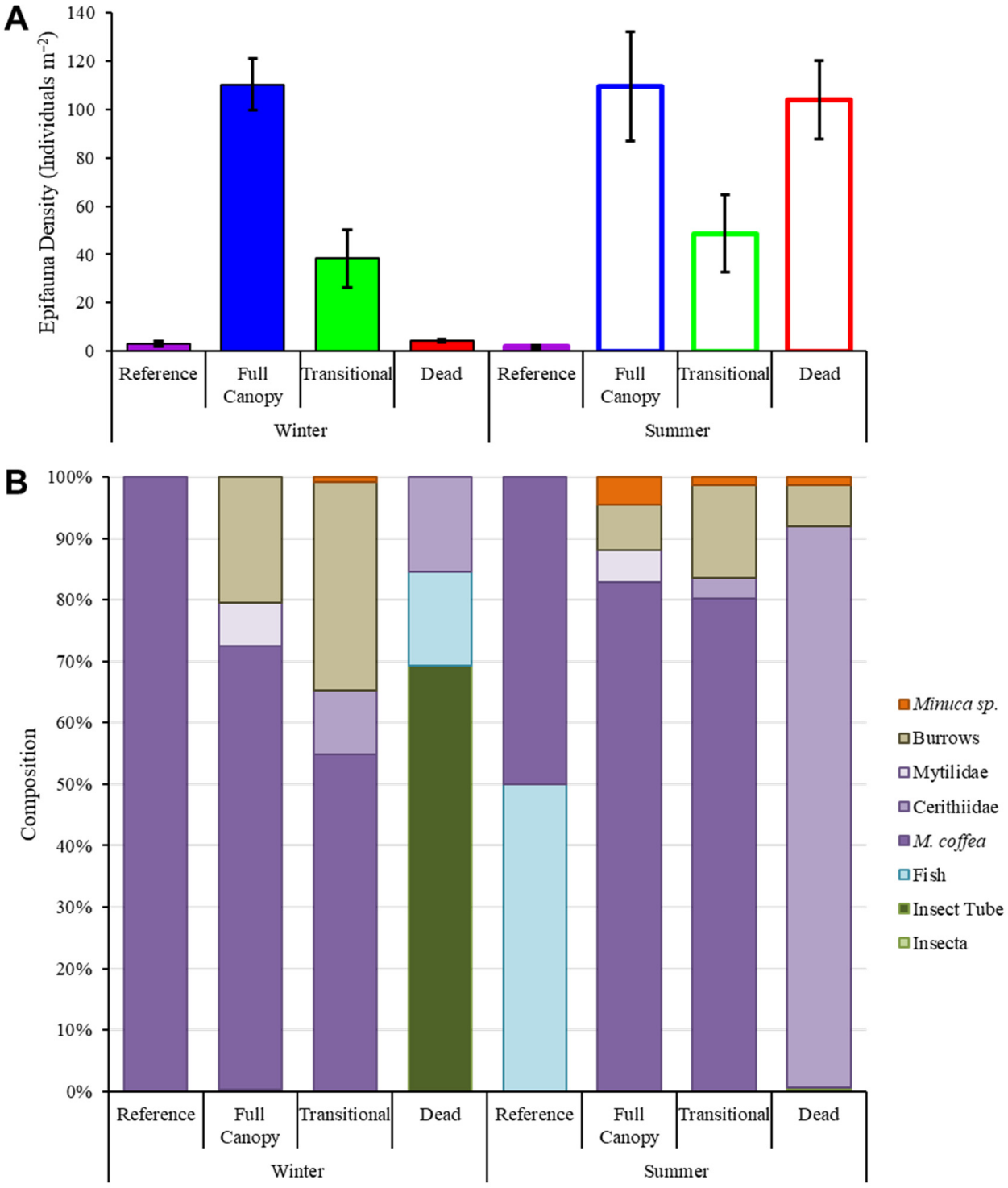

Figure 3. (**A**) Epifauna and biogenic structure density (individuals m^{-2}) ± 1 standard error and (**B**) taxonomic composition in surface quadrats during winter (January) and summer (August) 2015 from reference, full canopy, transitional, and dead zones. Colors in composition figure (**B**) represent major taxonomic groups: Mollusca (purple), insects (green), crabs (orange), fish (light blue), and burrows (beige).

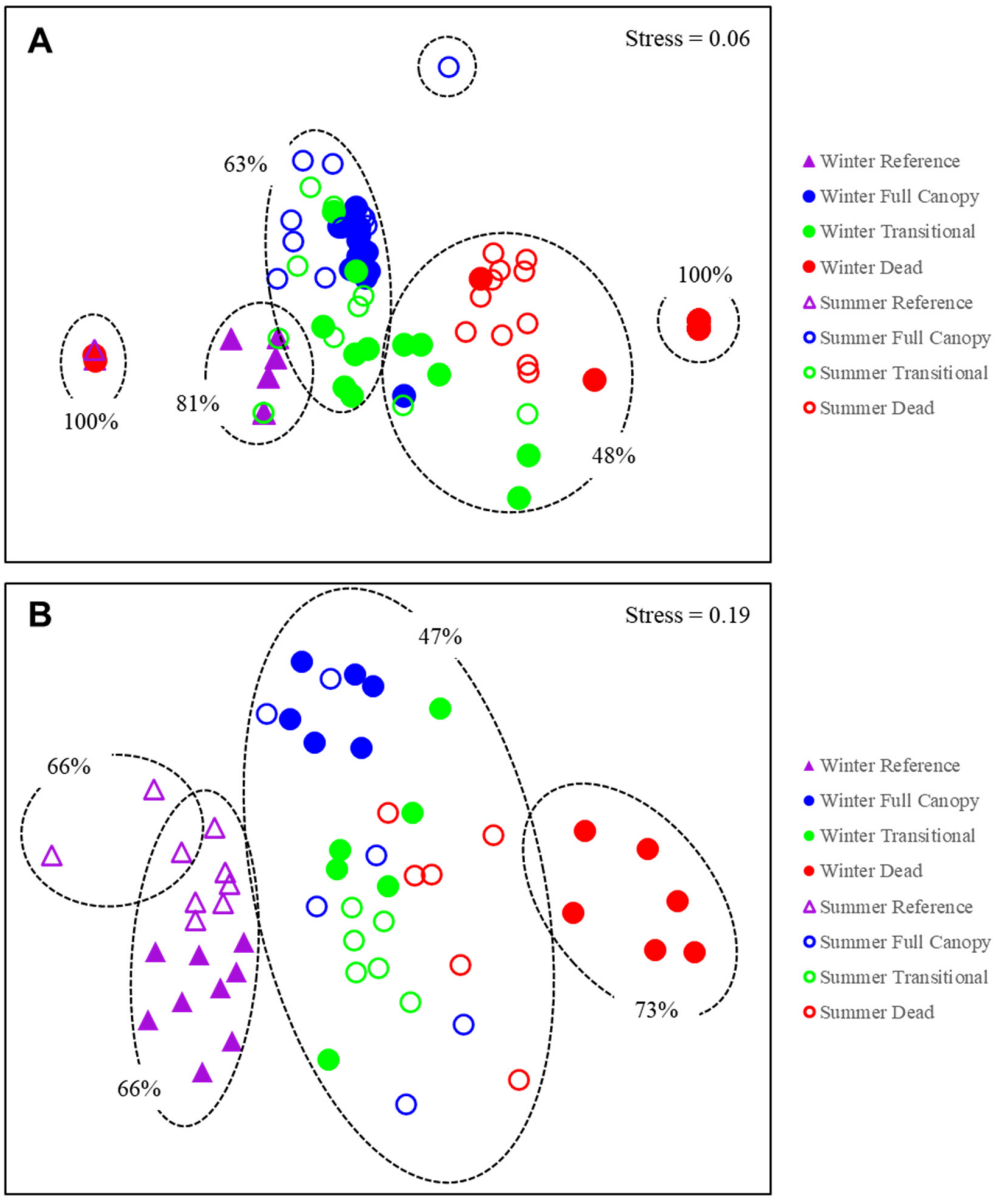

Figure 4. A non-metric multidimensional scaling plot for (**A**) epifauna and (**B**) infauna in the surface sediments collected during winter (January, solid symbols) and summer (August, open symbols) of 2015 based on Bray–Curtis similarities of square root-transformed density data. The colors refer to the zones: purple = reference; blue = full canopy; green = transitional; red = dead. The ellipses represent significant clusters with average similarity among the cluster samples indicated.

3.2.2. Infauna

A total of 5655 individuals were collected from the sediment cores across both time points and zones. Of the 34 taxa observed, 7 were present across all the zones, including Capitellidae, Nereididae, Tubificinae, Cochliopidae, Ceratopogonidae larvae, Acari, and Turbellaria (Supplemental Table S5), while 17 were present within only one zone. The full canopy zone contained the highest number of unique infaunal taxa (10), including Fabriciidae, Orbiniidae, Enchytraeidae, Mytilidae, and Cyrenoididae, followed by transitional with 3 unique taxa. The reference and dead zones had the least number of unique taxa (two and one, respectively) and overall taxa (Table 2). A significant interaction was detected in the macrofaunal densities, as well as for Shannon diversity (H'log$_e$) (Table 2) between time and zone (Supplemental Table S2). The dead zone had the highest densities and lowest diversity (H') and evenness (J') compared to all the other zones for winter. In contrast, these

metrics were similar between time points within the transitional, full canopy, or reference (Supplemental Table S2) zones. H′ was also lower in the reference than in the full canopy and transitional zones (Supplemental Table S2) for both time points.

Taxonomic composition varied both temporally and among zones (Figure 5, Supplemental Table S3) based on SIMPER analysis. The infaunal communities from the dead zone were most distinct from the reference zone (Similarity: 22.9%), followed by the full canopy (Similarity: 29.5%) and the transitional zones (Similarity: 37%). Dead zone infauna was dominated by Insecta (Ceratopogonidae) in the winter and Capitellidae and Oligochaeta in the summer. Ceratopogonidae and Dolichopodidae larvae (Insecta) had higher densities in the dead zone, whereas the transitional and full canopy zones were dominated by Oligochaeta in both time points. During the winter, the transitional zone had higher densities of Capitellidae and Tubificinae, while Capitellidae and Orbiniidae were more prevalent in the full canopy zone. In contrast, the reference zone was dominated by higher proportions of Insecta (e.g., Chironomidae) and Mollusca (e.g., Cochliopidae). Summer was characterized by higher densities of Cochliopidae (Gastropoda) and Turbellaria in the transitional zone, Ceratopogonidae larvae, Tubificinae, and Syllidae in the full canopy zone, and higher densities of Tubificinae in the reference zone.

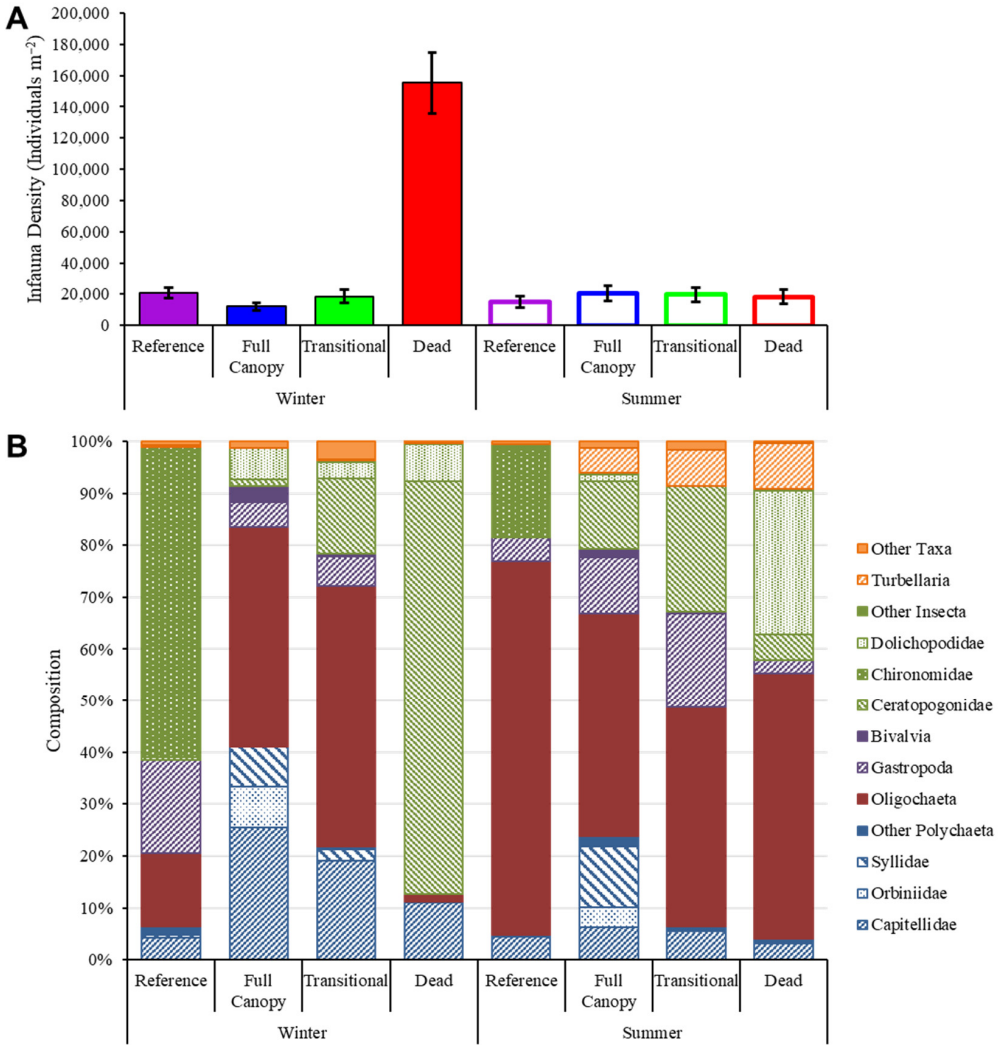

Figure 5. (**A**) Infauna density (individuals m^{-2}) ± 1 standard error and (**B**) taxonomic composition in the upper 2 cm of sediment during winter (January) and summer (August) 2015 from reference, full canopy, transitional, and dead zones. Colors in composition figure (**B**) represent major taxonomic groups: Polychaeta (dark blue), Oligochaeta (red), Mollusca (purple), insects (green), and other taxa (orange).

Cluster analysis identified four groups based on the infaunal communities (Figure 4B). The winter dead communities composed their own group with 73% similarity due to similar densities of Ceratopogonidae and Dolichopodidae larvae. The summer dead communities clustered with all of the full canopy and transitional communities (47% similarity) due to similar densities of Tubificinae, Ceratopogonidae, and Capitellidae. All of the reference communities fell into two groups: the first was composed of three summer samples at 66% similarity due to similar densities of Chironomidae and Tubificinae, and the remaining samples grouped together (66% similarity) with the addition of Cochliopidae. The infaunal community structure was significantly correlated to the observed epifaunal communities within the associated quadrats (RELATE, rho = 0.4, $p = 0.0001$), which may indicate that both communities are influenced by similar environmental drivers.

3.3. Environmental Drivers of Community Patterns

Several environmental variables were the potential drivers of epifaunal community variability (Table 3, $p = 0.001$–0.046). The "best" model included $\delta^{13}C$, porewater temperature, percent oxygen (O_2%), sand content, light, and *R. mangle* prop roots explaining 53.6% of the variation in epifauna (Table 3, Figure 6A). The dbRDA1 axis mostly separated the dead zone from the other zones, due to higher $\delta^{13}C$ and light values. The dbRDA2 axis was largely influenced by *R. mangle* roots, sand content, O_2%, and porewater temperature, distinguishing the transitional, full canopy, and reference zones and associated time points. All the top 10 models were within 1 AICc of the top model, with $\delta^{13}C$ as a common variable present in all the models and temperature included in 9 out of 10 models; notably, one model included sediment $\delta^{15}N$ as another potential discriminating factor (Table 3).

Table 3. Results from distance-based linear modeling (DistLM) for environmental variables with epifaunal communities. Values in bold indicate significant individual variables.

Variable	SS (Trace)	Pseudo-F	*p*-Value	Proportion
$\delta^{13}C$	**33,181**	**15.09**	**0.001**	**0.301**
%C	3745	1.23	0.298	0.034
$\delta^{15}N$	**20,777**	**8.14**	**0.001**	**0.189**
%N	6544	2.21	0.072	0.059
C:N	**16,636**	**6.23**	**0.001**	**0.151**
Biomass (B)	**24,259**	**9.89**	**0.001**	**0.220**
Light	**21,775**	**8.62**	**0.001**	**0.198**
Pneumatophores (Pneu)	**17,233**	**6.49**	**0.001**	**0.156**
Avicennia germinans Seedlings (*Ag*)	4748	1.58	0.153	0.043
***Rhizophora mangle* Roots (*Rm*)**	**6880**	**2.33**	**0.046**	**0.062**
Surface Salinity (SS)	4600	1.53	0.191	0.042
Salinity—30 cm (S)	3025	0.99	0.438	0.027
Temperature—30 cm (T)	5541	1.85	0.121	0.050
% O_2—30 cm (%O_2)	2498	0.81	0.504	0.023
O_2 (mg/L)—30 cm (O_2)	2094	0.68	0.644	0.019
Conductivity—30 cm (C)	3334	1.09	0.365	0.030
% Sand	6232	2.10	0.071	0.057
Eh—5 cm (Eh5)	5480	1.83	0.112	0.050
Eh—15 cm (Eh15)	6963	2.36	0.052	0.063
Eh—30 cm (Eh30)	3274	1.07	0.362	0.030
Total	110,150			

Table 3. *Cont.*

AICc	R^2	RSS	Selections
285.41	0.536	51,123	$\delta^{13}C$, T, $\%O_2$, % Sand, Light, *Rm*
285.77	0.491	56,080	$\delta^{13}C$, T, $\%O_2$, % Sand, Light
285.8	0.491	56,113	$\delta^{13}C$, T, $\%O_2$, % Sand, *Rm*
285.89	0.448	60,789	$\delta^{13}C$, T, Light, *Rm*
285.93	0.489	56,315	$\delta^{13}C$, T, $\%O_2$, Light, *Rm*
286.03	0.446	61,007	$\delta^{13}C$, T, $\%O_2$, % Sand
286.05	0.487	56,499	$\delta^{13}C$, $\delta^{15}N$, T, Light, *Rm*
286.11	0.486	56,593	$\delta^{13}C$, T, % Sand, Light, *Rm*
286.21	0.401	65,926	$\delta^{13}C$, % Sand, Light
286.24	0.443	61,361	$\delta^{13}C$, T, $\%O_2$, *Rm*

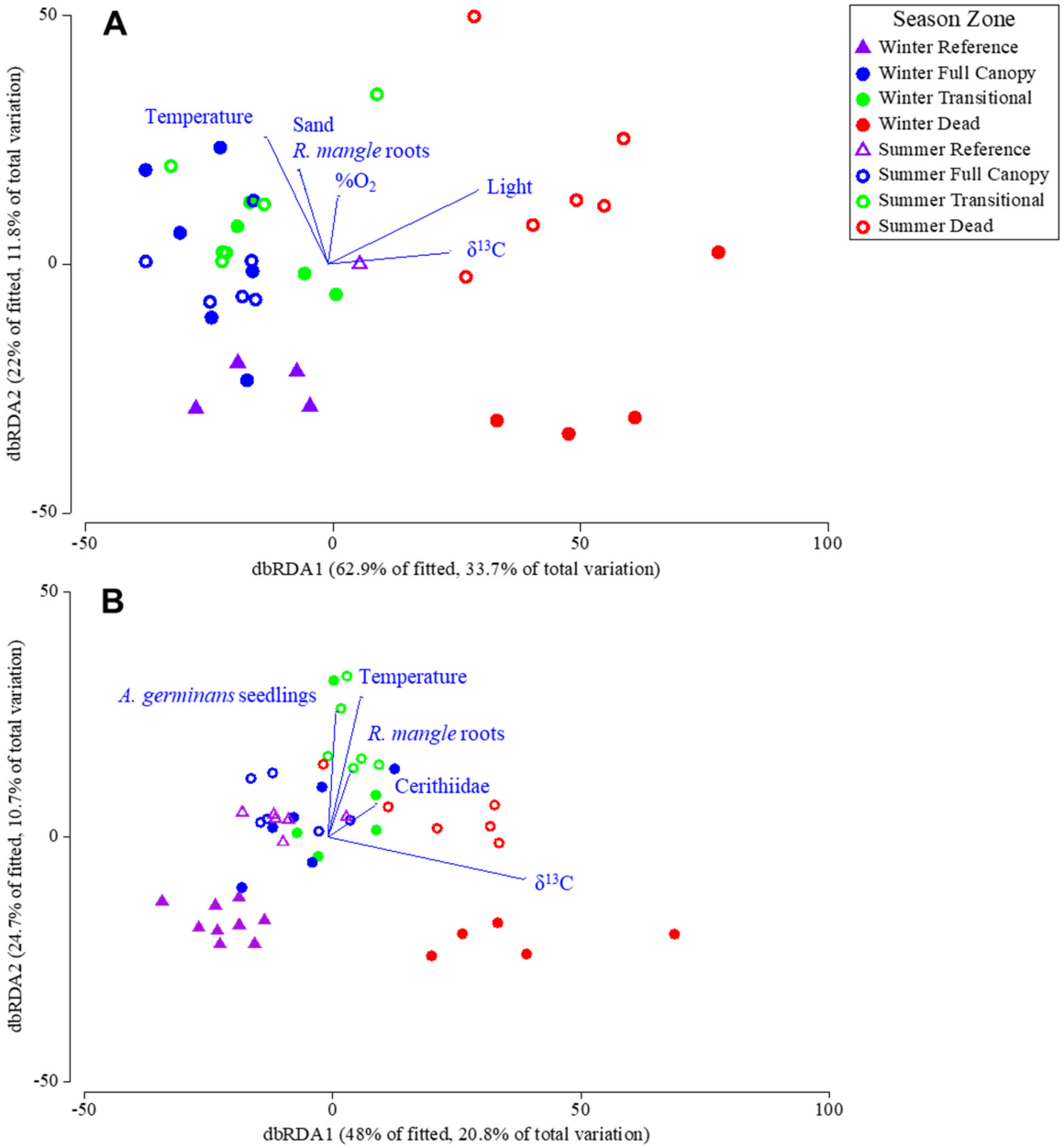

Figure 6. Distance-based redundancy analysis (dbRDA) of the "best" model from the distance-based linear modeling of the sampling locations within the zones based on Bray–Curtis similarities of square root-transformed (**A**) epifauna and (**B**) infauna density data.

Thirteen of the twenty-two environmental and biological variables individually accounted for a significant amount of the variation in the infaunal community structure, capable of explaining 5.4–17.8% of the variation (DistLM, p = 0.001–0.019, Table 4) and many were consistent with those identified for epifaunal communities (e.g., sediment $\delta^{13}C$, $\delta^{15}N$, C:N, belowground biomass, light levels, pneumatophores, and *R. mangle* prop roots). Pneumatophores (11%), insect tubes (13.6%), sediment $\delta^{15}N$ (16.9%), and $\delta^{13}C$ (17.8%) individually explained the greatest amounts of variation. Eleven of these thirteen variables were also components of the top 10 "best" models, while only light (7.5%) and belowground biomass (6%) were not included in any of the top 10 models. The "best" model included sediment $\delta^{13}C$, porewater temperature (T) at 30 cm, Cerithiidae (Ce), *A. germinans* seedlings (*Ag*), and *R. mangle* prop roots (*Rm*) explaining 43.3% of the community variation (Table 4, Figure 6B). The dbRDA1 axis was primarily influenced by sediment $\delta^{13}C$, as was observed for the epifaunal communities, with higher values separating the dead zone from the rest of the zones. The dbRDA2 axis was influenced by the porewater temperature, Cerithiidae, *R. mangle* roots, and *A. germinans* seedlings, separating winter from summer sampling time points. All of the top ten DistLM models were within the 1 AICc of the "best" model, including a seven-variable model that explained 48.6% of the community variation, incorporating insect tubes (ITs) and porewater conductivity (C) at 30 cm (Table 4).

Table 4. Results from distance-based linear modeling (DistLM) for environmental variables with infaunal communities. Values in bold indicate significant individual variables.

Variable	SS (Trace)	Pseudo-F	*p*-Value	Proportion
$\delta^{13}C$	**16,717**	**10.16**	**0.001**	**0.178**
% C	1428	0.72	0.677	0.015
$\delta^{15}N$	**15,937**	**9.59**	**0.001**	**0.169**
% N	3004	1.55	0.132	0.032
C:N	**6381**	**3.42**	**0.004**	**0.068**
Biomass (B)	**5599**	**2.97**	**0.011**	**0.060**
Insect Tubes (IT)	**12,820**	**7.42**	**0.001**	**0.136**
Cerithiidae (Ce)	**5392**	**2.86**	**0.015**	**0.057**
Light	**7009**	**3.78**	**0.003**	**0.075**
Pneumatophores (Pneu)	**10,343**	**5.81**	**0.001**	**0.110**
***Avicennia germinans* Seedlings (*Ag*)**	**5049**	**2.67**	**0.019**	**0.054**
***Rhizophora mangle* Roots (*Rm*)**	**6581**	**3.54**	**0.002**	**0.070**
Surface Salinity (SS)	3816	1.99	0.070	0.041
Salinity—30 cm (S)	3327	1.72	0.113	0.035
Temperature—30 cm (T)	**6769**	**3.64**	**0.001**	**0.072**
% O_2—30 cm (%O_2)	3313	1.72	0.093	0.035
O_2 (mg/L)—30 cm (O_2)	1245	0.63	0.759	0.013
Conductivity—30 cm (C)	**6839**	**3.69**	**0.003**	**0.073**
% Sand	**6885**	**3.71**	**0.001**	**0.073**
Eh—5 cm (Eh5)	2834	1.46	0.188	0.030
Eh—15 cm (Eh15)	2747	1.41	0.181	0.029
Eh—30 cm (Eh30)	3023	1.56	0.159	0.032
Total	94,057			

AICc	R^2	RSS	Selections
356.56	0.434	53,260	$\delta^{13}C$, T, Ce, *Ag*, *Rm*
356.75	0.462	50,558	$\delta^{13}C$, T, C, Ce, *Ag*, *Rm*
356.86	0.430	53,581	$\delta^{13}C$, T, IT, *Ag*, *Rm*
357.22	0.457	51,051	$\delta^{13}C$, T, C, IT, *Ag*, *Rm*
357.24	0.457	51,071	$\delta^{13}C$, T, IT, *Ag*, *Rm*
357.28	0.457	51,109	$\delta^{13}C$, $\delta^{15}N$, T, Ce, *Ag*, *Rm*
357.41	0.455	51,251	$\delta^{13}C$, T, Eh30, *Ag*, *Rm*
357.44	0.486	48,364	$\delta^{13}C$, T, C, IT, Ce, *Ag*, *Rm*
357.48	0.454	51,323	$\delta^{13}C$, C:N, T, Ce, *Ag*, *Rm*
357.56	0.422	54,350	$\delta^{13}C$, T, % Sand, Ce, *Rm*

3.4. Zonation in Mangrove Trophic Ecology

A total of 811 samples were analyzed for $\delta^{13}C$ and $\delta^{15}N$ (Supplemental Table S6), including surface sediments, POM, other primary producers (algae, benthic microalgae, *Batis maritima*, and mangrove leaves) and fauna (four phyla). The $\delta^{13}C$ values of the primary producers differed by zone and season, whereas while the $\delta^{15}N$ values for the producers varied by zone, there were no temporal patterns evident (Supplemental Table S2). The primary producers from the reference, full canopy, and transitional zones sites were ^{13}C-depleted compared to the dead zones in both time points (Supplemental Figure S1). In the summer, the primary producers from the full canopy zone were ^{13}C-depleted compared to the dead and transitional zones. While the primary producer $\delta^{15}N$ values where similar for the winter collections, the summer collections from the reference zone had significantly lower $\delta^{15}N$ values compared to the full canopy and transitional zones. POM was collected opportunistically where surface water was available and was not specific to a particular zone; the corresponding isotope values did not differ over time.

The isotopic niche space estimated using SEA_c and SEA_b, and the isotope centroid locations differed among the zones and time points (Figure 7; Tables 5 and 6). The fauna from the dead zone had significantly higher SEA_c and SEA_b values compared to all the other zones in the winter (Figure 7, Table 5). The dead zone also had higher CR, NR, CD, MNND, and SDNND than most of the other zones sampled in winter, indicating a higher diversity of the available carbon resources utilized (CR), potentially longer food chains or trophic length (NR), and overall higher trophic diversity (CD). Likewise, the higher MNND values in the dead zone may suggest higher diversity and less trophic redundancy compared to the full canopy and reference zones, while the higher SDNND values suggest a less even distribution of isotopic niches. In the winter, the full canopy (blue) and reference (purple) zones had similar SEA_c and SEA_b areas (Figure 7, Table 5); however, the ellipse orientations differed, and the small degree of overlap reflects this pattern (Figure 7, Table 6). The reference zone had a larger variation in the $\delta^{13}C$ values relative to $\delta^{15}N$ values, whereas the full canopy ellipse was tilted due to similar variations in both the $\delta^{13}C$ and $\delta^{15}N$ values (Figure 7). For the summer, all the zones had higher SEA_b compared to the reference zone. Temporal patterns were also evident for the reference zone for CR, NR, MNND, and SDNND, including a greater diversity of food resources (CR) and less even distribution of isotopic niches (SDNND) in winter, but higher diversity in trophic length (NR) and trophic diversity (MNND) in summer. While all the isotopic niche metrics for the dead zone decreased in the summer (Table 5), MNND remained higher than the full canopy and transition zones, indicating the overall trophic diversity was maintained in the dead zone over time. There was also a decrease in ellipse area overlap (Table 6) between winter and summer for the dead zone and all the other zones, indicating further distinction in the isotopic niche space occupied by the dead zone community. In contrast, there were no clear temporal patterns in CR, NR, MNND, and SDNND for the full canopy zone, indicating consistency in the trophic diversity through time.

Table 5. Isotopic niche area (‰^{2}) estimates (sample size-corrected standard ellipse area, SEA_c and Bayesian SEA, SEA_b), including 95% credible intervals (CIs) for fauna collected in 4 habitat zones: (R)eference, (F)ull Canopy, (T)ransitional, and (D)ead during (W)inter and (S)ummer of 2015. CR = $\delta^{13}C$ range; NR = $\delta^{15}N$ range; CD = centroid distance; MNND = mean nearest neighbor distance; SDNND = standard deviation of nearest neighbor distance. Values in bold represent significant differences between zones and * designate differences within zones between winter and summer based on a < 0.05 for posterior distribution (PD) comparisons.

Time	Zone	n	SEAc	SEAb	95% CI	PD	CR	PD	NR	PD	CD	PD	MNND	PD	SD NND	PD
W	R	63	7.25	7.168	6.57/7.80		3.91 *		2.36		1.89		1.55		1.06 *	
	F	50	7.58	7.622	6.94/8.41		3.10		**3.81**	**F > R, T**	2.01		0.96		0.12	
	T	41	9.61	9.574	8.58/10.63		2.78		1.91		1.42		**2.09**	**T > F**	0.21	
	D	50	19.08	**18.94**	17.17/20.83	**D > R, F, T**	**5.64** *	**D > R, F, T**	**3.82**	**D > R, T**	**2.49** *	**D > R, F, T**	**2.78**	**D > R, F**	**1.50** *	**D > F, T**

Table 5. *Cont.*

Time	Zone	n	SEAc	SEAb	95% CI	PD	CR	PD	NR	PD	CD	PD	MNND	PD	SD NND	PD
S	R	92	6.76	6.77	6.28/7.22		2.58		**3.63** *		1.69		**2.27** *	**R > T, F**	0.05	
	F	56	10.31	**10.47**	9.47/11.35	**F > R**	**3.45**	**F > D**	3.48		**2.16**	**F > D, R**	0.83		0.29	
	T	63	12.48	**12.63**	11.43/13.62	**T > R**	**4.41** *	**T > D, F, R**	**3.32** *		1.93		1.23		0.88	
	D	53	14.18	**14.15**	12.70/15.38	**D > R**	2.51		3.19		1.68		**2.39**	**D > F, T**	0.76	

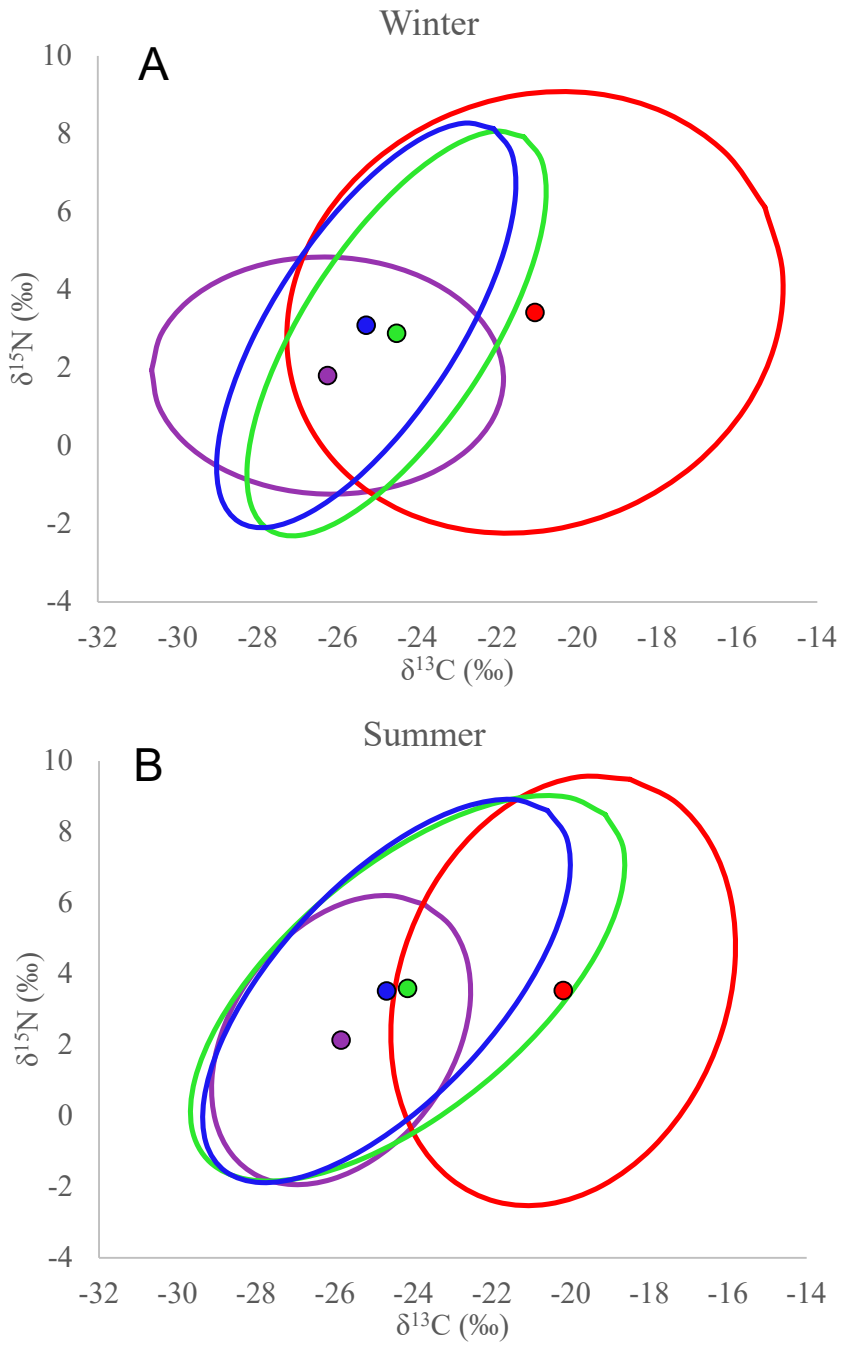

Figure 7. Fauna stable isotope data ($\delta^{13}C$ and $\delta^{15}N$, ‰, solid symbols represent centroids) and their corresponding standard ellipse area (SEA_c) for each habitat zone in (**A**) winter and (**B**) summer. Colors refer to zones: purple = reference; blue = full canopy; green = transitional; red = dead.

Table 6. Proportion of overlap in SEA_c and SEA_b (mean and 95% credible intervals) between different habitat zones based on fauna collected in winter (January) and summer (August) of 2015.

	Winter		Summer	
	SEA_c	SEA_b	SEA_c	SEA_b
Comparison		**Mean (95% CI)**		**Mean (95% CI)**
Dead vs. Transitional	47.80	46.16 (41.90/50.92)	36.60	35.94 (31.34/39.33)
Dead vs. Full Canopy	34.60	33.10 (29.45/36.53)	25.20	24.75 (21.58/27.79)
Dead vs. Reference	25.90	25.56 (21.86/28.98)	9.50	9.057 (6.82/10.79)
Transitional vs. Full Canopy	41.90	39.42 (36.18/41.80)	60.90	59.18 (55.17/62.46)
Transitional vs. Reference	32.10	31.52 (29.28/33.71)	40.00	38.47 (36.18/40.33)
Full Canopy vs. Reference	27.40	27.20 (24.74/29.64)	39.00	37.16 (35.16/39.15)

4. Discussion

4.1. Influence of Habitat Degradation on Sediment Characteristics

Natural mangrove habitats can exhibit stable, yet often extreme environments, with tidal flow supporting the consistent presence of mangrove trees and fauna. Changes in environmental factors like light, temperature, and precipitation occur seasonally, with extreme conditions occurring during summer when light and temperatures are at their peak [47,48]. When mangrove habitats degrade, they experience marked changes in their belowground and aboveground characteristics, consequently influencing ecosystem functioning. The limited vegetation, shade, and reduced tidal flushing typically present in degraded mangroves lead to more extreme environmental conditions, including intense sun exposure, higher temperatures, and lower percentages of oxygen [49–51]. In this study, the distinct environmental characteristics evident in the dead zone, namely the higher light conditions and sediment $\delta^{13}C$ values and lower C:N values were aligned with changes in the dominant sources of organic matter. The high light values were largely due to the reduced canopy cover and prop roots, consistent with both lower belowground biomass (i.e., the decline in the available mangrove root material) and lower redox values, potentially a consequence of less hydrological exchange and reduced flushing [5]. Higher light availability promotes the photosynthetic production of benthic microalgae and macroalgae, which is consistent with the lower sediment C:N values and higher sediment $\delta^{13}C$ values. As mangrove habitats degrade from full canopy to dead forests, dominant carbon sources likewise shift from C3 dominant mangrove detritus (^{13}C-depleted organic matter) that is more refractory in nature, inferred by the higher C:N values, to more labile algae that utilize different photosynthetic pathways [52] and can thrive in the high light conditions present in the dead zone. Degraded mangrove habitats are typically associated with lower organic content [18,53], reduced above- and belowground biomass, and variable sediment grain size [22] relative to healthy mangroves. While the sediment % organic carbon from the dead zones in this study did not differ from the other zones, this may be due to the different capacity to retain organic matter, recent degradation of the forest, and persistence of belowground carbon storage through compaction [8], and/or the contribution of algal organic matter replacing the relative proportion of mangrove detritus present in the other zones. However, there were clear zonation patterns in the isotopic composition of the available primary producers that shifted over time (Supplemental Figure S1), suggesting temporal changes in dominant carbon sources in degraded mangroves, which can influence ecosystem function (cf. [35]).

4.2. Influence of Mangrove Degradation on Benthic Faunal Community Structure

Mangroves are well-established ecosystem engineers, whereby their physical presence helps shape the environmental and biological structure of their faunal community [53]. Vegetation presence, in the form of seedlings and prop roots and reflected in the sediment $\delta^{13}C$ values, is a clear driver that directly and indirectly influences the composition and structure of mangrove faunal communities (Figure 6, Tables 3 and 4), evident from other

coastal wetlands [35,53–55]. Other vegetation, like *Batis maritima*, can also improve belowground structure, providing elevation to reduce inundation periods, leading to more stable temperatures and improved redox conditions [56]. The plant community creates structure, influencing the amount of shade and light present, sediment composition, overall sediment temperature, and substrate for epifauna, all of which were key structuring variables for the faunal communities. The extreme environmental conditions present in the dead zone, including higher temperatures, likely influence the lower faunal diversity and dominance by a few opportunistic taxa with broad tolerances. For example, the shift in the dominance of Ceratopogonidae larvae and pupae in the winter to Tubificinae oligochaetes and Capitellidae polychaetes during the more extreme summer environment is likely a consequence of differences in faunal environmental tolerances, as well as their respective life histories (cf. [57]). Because Ceratopogonidae larvae have limited nutritional reserves, their development often occurs in organic-rich mud [58]. The presence of BMA in the dead zone sediments and higher organic carbon content (winter) may provide suitable food resources for these larvae. While we were unable to analyze these larvae in the winter, their stable carbon and nitrogen isotope values (−16.2‰ and 1.9‰, respectively) from the summer are consistent with consuming ^{13}C-enriched organic matter, likely derived from BMA. These larvae also demonstrate developmental differences across seasons [58], with the winter months extending the larval stage and resulting in multiple generations of larvae occupying an area, whereas in the summer the larvae mature faster. Thus, the higher prevalence of larvae in the winter and reduced densities in the summer may reflect this seasonal gradient in time to maturity. In contrast, *Capitella* spp. and oligochaetes have adapted to tolerate high organic concentrations, including pollutants, low oxygen, and extreme salinities, and can reproduce rapidly once conditions improve [59]; thus, their dominance in summer may reflect their broad environmental tolerances and r-selected strategies.

Additional seasonal effects in south Florida may also be driving community differences. The summer months yield higher temperatures and more precipitation, peaking in August/September [47], and the dead zone offers little protection from these extrema. Storm events can lead to increased standing and flowing water, which is not hospitable to Ceratopogonidae larvae given that they cannot move well in water [58]. However, these conditions can support higher oligochaete abundances [60], given their broad environmental tolerances (e.g., [53]). Storm-induced erosional forces influence the movement and distribution of sediment particles, including the increased settlement of sand from suspended material [22,61] possibly from runoff. The larger sand particles, present in summer sediments, retain less organic matter relative to muddy sediments, which may also limit insect larval abundances. Summer precipitation events may disrupt the sediment surface and enhance erosion due to a lack of vegetation in the dead zone, further reducing sediment stability. Runoff can also transport pollutants in the form of high concentrations of organic material, leading to decreased oxygen coupled with increased nutrient loading and other contaminants. As a result, species with the ability to live in variable sediment types, as well as rapidly colonize areas with higher disturbance frequency, such as Tubificinae and Capitellidae, will dominate the community [22,59,60].

As shade, temperature, and increased root systems encourage biogeochemical reactions and physical structure, both known to affect benthic fauna densities and composition [11,22,62–64], it is not surprising that the models for both infauna and epifauna communities identified temperature and *R. mangle* roots as driving forces influencing faunal communities, in addition to δ^{13}C values (proxy tracer for dominant carbon and food resources). Mangrove faunal communities are often composed of decapod crustaceans, gastropods, polychaetes, oligochaetes, and insect larvae [20], as was observed in our study area; however, the specific faunal composition shifted along the zonation gradient. For example, Mollusca taxa composition changed with increasing mangrove canopy, which can be related to increased organic material available in the form of leaf litter for gastropods to consume, consistent with previous studies [27,65,66]. In the current study, Cerithiidae dominated the dead zone in both seasons, but these taxa were replaced by *Melampus coffea* in the

transition and full canopy zones. This detritivorous snail prefers higher soil organic matter and lower interstitial salinity [67]. The full canopy zone also supported bivalve molluscs, including *Geukensia granosissima*, known to be suspension feeders; these were found in small depressions at the base of *R. mangle* prop roots, submerged in standing water, which facilitates suspension feeding.

While changes were evident in the zones along the degradation gradient in the restoration area (T1 and T2), comparisons to a healthy natural mangrove provide insights into the status of restoration efforts and whether the restored areas are achieving functional equivalency to natural mangrove habitats. With dense coverage and thick foliage, the reference site provided consistent shade and predation protection to support an established epifaunal community dominated by *M. coffea*, with limited change over time. In contrast, the temporal changes in the diversity and composition of the infaunal communities indicate they may be more sensitive to changes in belowground environmental controls than their epifaunal counterparts. In the winter, the dominance of Chironomidae larvae (Figure 5B) is consistent with their preference for habitats with abundant organic matter for food [68] and dense root structures that can offer predation protection [69]. The mature mangrove forest (reference) provides a constant supply of fresh organic matter that can support larvae for extended time periods, resulting in higher densities (cf. [68]). In contrast, the changes in community dominance from winter to summer, including the increased prevalence of oligochaetes, may be linked to changes in precipitation with insects dominating drier periods (winter) and oligochaetes in periods of higher precipitation (summer) due to differing life histories and respective larval dispersal modes [60]. Thus, given there were clear changes in infaunal communities between these two time points in the reference site, monitoring these communities at multiple time points helps to decouple natural variability from further change, either decline or recovery, in the degraded mangrove areas.

4.3. Mangrove Degradation Gradient Aligns with Shifts in Trophic Structure and Function

Community-wide metrics revealed diverse food webs that were distinct by zone and time points, with the size of the stable isotope space that is occupied by consumers representing their trophic diversity (Figure 7, Table 5) and the degree of species packing (i.e., consumers with similar isotope values) in this space reflecting relative trophic redundancy [35]. For example, the dead zone exhibited high trophic diversity but lower trophic redundancy overall, suggesting that this zone is highly dynamic and potentially vulnerable to change. With the limited overlap among SEA between the dead and other zones (Figure 7, Table 6), the trophic diversity of the consumers residing in the dead zone may reflect relative maturity, or immaturity in this case, of the mangrove ecosystem (cf. [23,35]). Specifically, the presence of particular primary producers, e.g., mangrove plants and/or BMA, can encourage modifications in the abiotic environmental conditions, which consequently influence the stable isotope values of primary producers. These bottom-up controls on primary producers can shape the development of consumer food webs [28,35,70]. For example, the $\delta^{13}C$ values of certain grazing molluscs, *Littoraria angulifera* and Cochliopidae snails, decreased with increased plant canopy cover, as inferred in SIA, from dead to reference (Supplemental Table S6). However, isotope trajectories for different trophic groups may be non-uniform or uneven, thus we chose to examine the overall community isotopic patterns rather than specific components, avoiding the potential conundrum of not having the same species represented in all the zones. The zonation pattern in the Mollusca isotopes was widespread across taxa and evident in the community-wide trophic niche space inferred from SEA_c and SEA_b ellipses (Figure 7; Table 5). Lower consumer $\delta^{13}C$ values track the ^{13}C-depleted characteristics of mangrove detritus [15,23,28], where changes in the mangrove leaf $\delta^{13}C$ values can also be a function of environmental stress [28]. As predicted, stable carbon isotopes shifted from lower $\delta^{13}C$ values in the mangrove-dominated reference and full canopy zones to higher $\delta^{13}C$ values in the algae-dominated dead zone (Ref. [15], this study [23]). Patterns in community-wide isotope metrics examined here help inform the

broader impacts of these shifting baselines, which can be a function of mangrove forest age, maturity, and degradation [23,28,53].

Temporal changes within and across zones were also evident in the trophic diversity metrics examined, indicating dynamic variations in the baseline carbon sources available and the assimilation of food sources within these environments over time. With the increased availability of micro- and macroalgae, the fauna collected in the summer may be more reliant on algae and less on the other available carbon sources (e.g., mangrove detritus) resulting in lower SEA_c and CR values and less SEA overlap with the other zones compared to the winter sampling (Figure 7, Tables 5 and 6). While mangrove trees and detritus were sparsely present in the dead zone, micro- and macroalgae may have been more consistently available relative to the other zones. Persistent high niche space occupied by the dead zone community suggests that the isotopic drivers of these communities may be less driven by season. Likewise, similarities in SEA size, position of the centroid, and high SEA overlap between transitional and full canopy zones, as well as the consistency in ellipse shape suggest stabilization in food webs, potentially reflecting similar resource availability for fauna residing in these zones. However, the composition of taxa residing in these zones was distinct (Figure 4), which may indicate some degree of trophic redundancy and functional equivalency in the trophic ecology of these zones.

Trophic succession with the maturing of wetlands, from either recovery following natural disturbance or direct restoration actions, typically follows the progressive increase in trophic guilds in concert with (or following some lag period) the increased availability of basal sources [35,70,71]. While the presence of multiple baseline food resources in mature mangroves might predict the diversification of energy pathways within a food web (cf. [30]), when a basal source becomes the dominant resource, as in the mature mangrove forest, and as algal sources become less prevalent due to increased canopy and shading, the food web may instead become more simplified (e.g., [30]). In the current study, the reference zone community metrics demonstrated a narrower range in the carbon and nitrogen isotope signal, possibly reflecting the simplification of the food web, corresponding to the dominance of and less variation in the isotopic composition of basal food resources, including the prevalence of mangrove-derived organic matter and less inclusion of macro- and microalgae basal sources. While SEA_c and SEA_b had consistent sizes between the time points, the reference zone demonstrated higher CR values and lower NR values in winter, which may reflect increased availability in baseline resources present (CR) and an overall reduction in the number of trophic levels and/or diversity of nitrogen sources in the wintertime (lower NR). In contrast, fewer carbon sources may be available in the summertime (lower CR), but more trophic levels and/or higher variation in the nitrogen isotopic composition are present, as indicated by the higher NR values. The increase in MNND values from winter to summer may indicate that summer communities were composed of more trophic complexity (inferred from higher MNND values). These results highlight the value of including appropriate reference sites in restoration studies given temporal changes were evident across isotope metrics (e.g., CR, NR, and MNND) and across zones. Future work that includes additional replicate reference sites and full canopy areas in proximity to restored mangroves could help to improve the ability to capture variation in time and space and minimize risk due to natural disturbance (e.g., hurricanes). This approach allows a decoupling of natural variation from changes in restored sites due to recovery or further decline.

Many factors influence isotopic dispersion and resulting zonation patterns in community-wide trophic metrics (e.g., [32]). These include variations in the isotope values of potential food resources, compositional changes in the consumers, and variations in their resource use (in both space and time) [30,35]. In the case of RBNERR, are all of these germane to this system? The abiotic environment within discrete habitats can directly or indirectly influence the primary producer's isotopic composition, which is then transferred up the food chain. For example, the fiddler crab, *Minuca rapax*, was present in nearly all the zones for both the time points. Its $\delta^{13}C$ composition (Supplemental Table S4) decreased from

dead to full canopy to reference zones (when present), potentially reflecting the shifting baseline isotopic composition of its primary food resources, likely detrital and algal pools. Similarly, this pattern was reported in the isotopic composition of grazing *L. angulifera*, with $\delta^{13}C$ values decreasing as the mangrove canopy increased. These isotopic patterns indicate changing $\delta^{13}C$ values of food resources [72]. Controls on BMA include light availability, temperature, and salinity, all of which structure microalgal communities and influence their photosynthetic rates and can directly impact their isotopic composition (e.g., [70]). Given the fauna analyzed in this study do not move over large areas, their feeding habits are spatially restricted, and thus their isotopic composition is linked to the physical and chemical conditions of their habitat, rather than shifting resource use over time. Hence, community metrics derived in this study reflect the localized feeding of fauna, consistent with spatially restricted trophic processes.

Consumer isotope values and community-wide metrics could reflect species-specific habitat affinity, given that infaunal and epifaunal communities differed by zone (Figure 4). In other words, if community structure is correlated to function, we could assume that the trophic function would be zone-specific because different communities were present in each zone [35]. However, there were only three taxa analyzed from the reference zone that were not included in the other zones at the taxonomic level identified. Given consistent taxa were analyzed for isotopes across zones in this study, different community compositions by zone (Figure 4) do not explain the isotopic niche separation among zones, nor necessarily equate to altered functionality of the overall system. By tracking the stable isotopic composition in specific consumer groups and the overall community with time, we can evaluate the relative importance certain taxa may play in shaping general trophic structure, whether in a degraded mangrove system or following wetland restoration.

As degraded mangroves recover, as observed in early successional wetlands, the macroinvertebrate food web is fueled by a "green" or algivore-dominated food web (cf. [23,35]), with BMA and cyanobacteria providing the primary baseline food resource. As different plants colonize and zonation develops, the successional sequence within the food web shifts from mostly microalgivore insect larvae grazing on algae at the sediment surface to detritivores (e.g., Oligochaeta) feeding at the sub-surface [73]. Tracking this successional sequence from green (grazers) to brown (decomposer-based) food webs is relatively cost-effective through traditional ecological sampling coupled with stable isotope analysis, as exemplified in this study. Monitoring the differing balance of green and brown consumer pathways provides a mechanism to track recovery trajectories in restored wetlands [35], including mangrove ecosystems. Specifically, measuring a subset of fauna from restored and reference mangroves on a regular basis (e.g., twice a year as in this study) to provide baseline metrics, with a supplementary sampling of more taxonomic groups less frequently (e.g., every 2–5 years), may help capture the short- and long-term changes in the trophic function of restored mangroves and associated timescales to achieve functional equivalency.

5. Conclusions

Traditional ecological monitoring techniques coupled with stable isotope community metrics can be used to track restoration success by measuring the recovery rates of benthic faunal diversity and trophic functioning. In the current study, epifaunal and infaunal community composition differed along a degradation gradient, consistent with mangrove forest structure influencing benthic community patterns. Stable isotopes helped identify key food resources and dominant trophic groups present at different mangrove successional stages, providing taxonomic and functional targets for restoration success. We also found that stable isotopes provide key information on spatial processes in mangrove habitats, including the ecological residency or connectivity among discrete habitats (zones). Thus, quantifying benthic community metrics coupled with stable isotopes and niche analysis support the evaluation of restoration actions by tracking changes in system responses, providing powerful tools to help understand recovery and resilience in coastal habitats.

Supplementary Materials: The following supporting information can be downloaded at https://www.mdpi.com/article/10.3390/d16110659/s1, Figure S1: Producer stable isotope data and their corresponding standard ellipse area for each habitat zone; Table S1: Statistical comparisons between T1 and T2 based on habitat zone; Table S2: Statistical comparisons among habitat zones and between time points from 2015 collections at Fruit Farm Creek; Table S3: Statistical comparisons among habitat zones within time points from 2015 collections at Fruit Farm Creek; Table S4: Epifauna and flora community metrics from quadrats examined during January and August in 2015; Table S5: Infauna community metrics from 2 cm sediment cores collected during January and August in 2015; Table S6: Summarized $\delta^{13}C$, $\delta^{15}N$ and C:N data for fauna, flora and POM collected in 2015 from Fruit Farm Creek.

Author Contributions: Conceptualization: A.W.J.D., J.R.B., K.W.K. and N.C.; methodology: A.W.J.D., J.R.B., J.P.M.-C. and N.C.; validation: A.W.J.D., J.R.B. and J.P.M.-C.; formal analysis: A.W.J.D., J.R.B. and J.P.M.-C.; investigation: A.W.J.D., J.R.B., J.P.M.-C., N.C. and K.W.K.; resources: A.W.J.D. and K.W.K.; writing—original draft preparation: A.W.J.D., J.R.B. and J.P.M.-C.; writing—review and editing: all authors; visualization: A.W.J.D., J.R.B. and J.P.M.-C.; supervision: A.W.J.D. and K.W.K.; project administration: A.W.J.D. and K.W.K.; funding acquisition: A.W.J.D. and K.W.K. All authors have read and agreed to the published version of the manuscript.

Funding: This research was funded by the USGS Land Management Research Program, project SC009HC, task 22.

Institutional Review Board Statement: Not applicable.

Data Availability Statement: Data presented are openly available [41].

Acknowledgments: We would like to thank Kevin Cunniff, Ashley King, and Megan Rasmussen for field assistance, as well as the late Roy R. "Robin" Lewis III for his work in mangrove restoration within this study area. Access to sites was facilitated by Rookery Bay National Estuarine Research Reserve and the private residential community, Key Marco, located on Horrs Island. We also thank two anonymous reviewers and Brian Fry for constructive comments that improved the final manuscript. Funding support was provided through the USGS Land Management Research Program. Any use of trade, firm, or product names is for descriptive purposes only and does not imply endorsement by the U.S. Government.

Conflicts of Interest: The authors declare no conflicts of interest.

References

1. Lee, S.Y.; Primavera, J.H.; Dahdouh-Guebas, F.; McKee, K.; Bosire, J.O.; Cannicci, S.; Diele, K.; Fromard, F.; Koedam, N.; Marchand, C.; et al. Ecological role and services of tropical mangrove ecosystems: A reassessment. *Glob. Ecol. Biogeogr.* **2014**, *23*, 726–743. [CrossRef]
2. Krauss, K.W.; McKee, K.L.; Lovelock, C.E.; Cahoon, D.R.; Saintilan, N.; Reef, R.; Chen, L. How mangrove forests adjust to rising sea level. *New Phytol.* **2014**, *202*, 19–34. [CrossRef] [PubMed]
3. Osland, M.J.; Spivak, A.C.; Nestlerode, J.A.; Lessmann, J.M.; Almario, A.E.; Heitmuller, P.T.; Russell, M.J.; Krauss, K.W.; Alvarez, F.; Dantin, D.D.; et al. Ecosystem development after mangrove wetland creation: Plant-Soil change across a 20-year chronosequence. *Ecosystems* **2012**, *15*, 848–866. [CrossRef]
4. Lovelock, C.E.; Duarte, C.M. Dimensions of blue carbon and emerging perspectives. *Biol. Lett.* **2019**, *15*, 20180781. [CrossRef]
5. Cormier, N.; Krauss, K.W.; Demopoulos, A.W.; Jessen, B.J.; McClain-Counts, J.P.; From, A.S.; Flynn, L.L. Potential for carbon and nitrogen sequestration by restoring tidal connectivity and enhancing soil surface elevations in denuded and degraded south Florida mangrove ecosystems. In *Wetland Carbon and Environmental Management*; Wiley: Hoboken, NJ, USA, 2022; pp. 143–158.
6. Duke, N.C.; Meynecke, J.O.; Dittmann, S.; Ellison, A.M.; Anger, K.; Berger, U.; Cannicci, S.; Diele, K.; Ewel, K.C.; Field, C.D.; et al. A world without mangroves? *Science* **2007**, *317*, 41–42. [CrossRef]
7. Spalding, M. *World Atlas of Mangroves*; Routledge: London, UK, 2010.
8. Krauss, K.W.; Demopoulos, A.W.J.; Cormier, N.; From, A.S.; McClain-Counts, J.P.; Lewis, R.R. Ghost forests of Marco Island: Mangrove mortality driven by belowground soil structural shifts during tidal hydrologic alteration. *Estuar. Coast. Shelf Sci.* **2018**, *212*, 51–62. [CrossRef]
9. Lewis, R.R.; Milbrandt, E.C.; Brown, B.; Krauss, K.W.; Rovai, A.S.; Beever, J.W.; Flynn, L.L. Stress in mangrove forests: Early detection and preemptive rehabilitation are essential for future successful worldwide mangrove forest management. *Mar. Pollut. Bull.* **2016**, *109*, 764–771. [CrossRef]
10. Duarte, C.M.; Dennison, W.C.; Orth, R.J.; Carruthers, T.J. The charisma of coastal ecosystems: Addressing the imbalance. *Estuaries Coasts* **2008**, *31*, 233–238. [CrossRef]

11. Sweetman, A.K.; Middelburg, J.J.; Berle, A.M.; Bernardino, A.F.; Schander, C.; Demopoulos, A.W.J.; Smith, C.R. Impacts of exotic mangrove forests and mangrove deforestation on carbon remineralization and ecosystem functioning in marine sediments. *Biogeosciences* **2010**, *7*, 2129–2145. [CrossRef]
12. Lewis, R.R. Ecological engineering for successful management and restoration of mangrove forests. *Ecol. Eng.* **2005**, *24*, 403–418. [CrossRef]
13. Lewis, D.B.; Brown, J.A.; Jimenez, K.L. Effects of flooding and warming on soil organic matter mineralization in *Avicennia germinans* mangrove forests and *Juncus roemerianus* salt marshes. *Estuar. Coast. Shelf Sci.* **2014**, *139*, 11–19. [CrossRef]
14. Radabaugh, K.R.; Dontis, E.E.; Chappel, A.R.; Russo, C.E.; Moyer, R.P. Early indicators of stress in mangrove forests with altered hydrology in Tampa Bay, Florida, USA. *Estuar. Coast. Shelf Sci.* **2021**, *254*, 107324. [CrossRef]
15. Then, A.Y.-H.; Adame, M.F.; Fry, B.; Chong, V.C.; Riekenberg, P.M.; Mohammad Zakaria, R.; Lee, S.Y. Stable isotopes clearly track mangrove inputs and food web changes along a reforestation gradient. *Ecosystems* **2021**, *24*, 939–954. [CrossRef]
16. Cannicci, S.; Burrows, D.; Fratini, S.; Smith, T.J.I.; Offenberg, J.; Dahdouh-Guebas, F. Faunal impact on vegetation structure and ecosystem function in mangrove forests: A review. *Aquat. Bot.* **2008**, *89*, 186–200. [CrossRef]
17. Nagelkerken, I.; Blaber, S.J.M.; Bouillon, S.; Green, P.; Haywood, M.; Kirton, L.G.; Meynecke, J.O.; Pawlik, J.; Penrose, H.M.; Sasekumar, A.; et al. The habitat function of mangroves for terrestrial and marine fauna: A review. *Aquat. Bot.* **2008**, *89*, 155–185. [CrossRef]
18. Carugati, L.; Gatto, B.; Rastelli, E.; Lo Martire, M.; Coral, C.; Greco, S.; Danovaro, R. Impact of mangrove forests degradation on biodiversity and ecosystem functioning. *Sci. Rep.* **2018**, *8*, 13298. [CrossRef] [PubMed]
19. Bianchi, T.S.; Aller, R.C.; Atwood, T.B.; Brown, C.J.; Buatois, L.A.; Levin, L.A.; Levinton, J.S.; Middelburg, J.J.; Morrison, E.S.; Regnier, P.; et al. What global biogeochemical consequences will marine animal–sediment interactions have during climate change? *Elem. Sci. Anthr.* **2021**, *9*, 00180. [CrossRef]
20. Lee, S.Y. Mangrove macrobenthos: Assemblages, services, and linkages. *J. Sea Res.* **2008**, *59*, 16–29. [CrossRef]
21. Barbanera, A.; Markesteijn, L.; Kairo, J.; Juma, G.A.; Karythis, S.; Skov, M.W. Functional responses of mangrove fauna to forest degradation. *Mar. Freshw. Res.* **2022**, *73*, 762–773. [CrossRef]
22. Bernardino, A.F.; Gomes, L.E.D.; Hadlich, H.L.; Andrades, R.; Correa, L.B. Mangrove clearing impacts on macrofaunal assemblages and benthic food webs in a tropical estuary. *Mar. Pollut. Bull.* **2018**, *126*, 228–235. [CrossRef]
23. Demopoulos, A.W.J.; Fry, B.; Smith, C.R. Food web structure in exotic and native mangroves: A Hawaii-Puerto Rico comparison. *Oecologia* **2007**, *153*, 675–686. [CrossRef] [PubMed]
24. Demopoulos, A.W.J.; Smith, C.R. Invasive mangroves alter macrofaunal community structure and facilitate opportunistic exotics. *Mar. Ecol. Prog. Ser.* **2010**, *404*, 51–67. [CrossRef]
25. Pardo, J.C.F.; Poste, A.E.; Frigstad, H.; Quintana, C.O.; Trannum, H.C. The interplay between terrestrial organic matter and benthic macrofauna: Framework, synthesis, and perspectives. *Ecosphere* **2023**, *14*, e4492. [CrossRef]
26. Bosire, J.O.; Dahdouh-Guebas, F.; Walton, M.; Crona, B.I.; Lewis, R.R.I.; Field, C.; Kairo, J.G.; Koedam, N. Functionality of restored mangroves: A review. *Aquat. Bot.* **2008**, *89*, 251–259. [CrossRef]
27. Salmo, S.G.; Tibbetts, I.; Duke, N.C. Colonization and shift of mollusc assemblages as a restoration indicator in planted mangroves in the Philippines. *Biodivers. Conserv.* **2017**, *26*, 865–881. [CrossRef]
28. Harada, Y.; Connolly, R.M.; Fry, B.; Maher, D.T.; Sippo, J.Z.; Jeffrey, L.C.; Bourke, A.J.; Lee, S.Y. Stable isotopes track the ecological and biogeochemical legacy of mass mangrove forest dieback in the Gulf of Carpentaria, Australia. *Biogeosciences* **2020**, *17*, 5599–5613. [CrossRef]
29. Fry, B.; Ewel, K.C. Using stable isotopes in mangrove fisheries research—A review and outlook. *Isot. Environ. Health Stud.* **2003**, *39*, 191–196. [CrossRef]
30. Quillien, N.; Nordström, M.C.; Schaal, G.; Bonsdorff, E.; Grall, J. Opportunistic basal resource simplifies food web structure and functioning of a highly dynamic marine environment. *J. Exp. Mar. Biol. Ecol.* **2016**, *477*, 92–102. [CrossRef]
31. Bouillon, S.; Connolly, R.M.; Lee, S.Y. Organic matter exchange and cycling in mangrove ecosystems: Recent insights from stable isotope studies. *J. Sea Res.* **2008**, *59*, 44–58. [CrossRef]
32. Layman, C.A.; Arrington, D.A.; Montana, C.G.; Post, D.M. Can stable isotope ratios provide for community-wide measures of trophic structure? *Ecology* **2007**, *88*, 42–48. [CrossRef]
33. Jackson, A.L.; Inger, R.; Parnell, A.C.; Bearhop, S. Comparing isotopic niche widths among and within communities: SIBER—Stable Isotope Bayesian Ellipses in R. *J. Anim. Ecol.* **2011**, *80*, 595–602. [CrossRef] [PubMed]
34. Powers, J.S.; Veldkamp, E. Regional variation in soil carbon and $\delta^{13}C$ in forests and pastures of northeastern Costa Rica. *Biogeochemistry* **2005**, *72*, 315–336. [CrossRef]
35. Nordström, M.C.; Demopoulos, A.W.J.; Whitcraft, C.R.; Rismondo, A.; McMillan, P.; Gonzalez, J.P.; Levin, L.A. Food web heterogeneity and succession in created saltmarshes. *J. Appl. Ecol.* **2015**, *52*, 1343–1354. [CrossRef]
36. Yando, E.S.; Sloey, T.M.; Dahdouh-Guebas, F.; Rogers, K.; Abuchahla, G.M.O.; Cannicci, S.; Canty, S.W.J.; Jennerjahn, T.C.; Ogurcak, D.E.; Adams, J.B.; et al. Conceptualizing ecosystem degradation using mangrove forests as a model system. *Biol. Conserv.* **2021**, *263*, 109355. [CrossRef]
37. Zysko, D.P.; Worley, K.; Lewis, R.R.I. *Fruit Farm Creek Mangrove Restoration Phase 1A Time Zero Monitoring Report*; The Ecology Group Inc.: Punta Gorda, FL, USA, 2012; p. 15.

38. McKee, K.L.; Mendelssohn, I.A.; Hester, M.W. Rexamination of pore water sulfide concentrations and redox potentials near the aerial roots of *Rhizophora mangle* and *Avicennia germinans*. *Am. J. Bot.* **1988**, *75*, 1352–1359. [CrossRef]
39. Moseman, S.; Levin, L.A.; Currin, C.; Fordera, C. Colonization, succession, and nutrition of macrobenthic assemblages in a restored wetland at Tijuana Estuary, California. *Estuar. Coast. Shelf Sci.* **2004**, *60*, 755–770. [CrossRef]
40. Demopoulos, A.W.J.; McClain-Counts, J.; Ross, S.W.; Brooke, S.; Mienis, F. Food-web dynamics and isotopic niches in deep-sea communities residing in a submarine canyon and on the adjacent open slopes. *Mar. Ecol. Prog. Ser.* **2017**, *578*, 19–33. [CrossRef]
41. Demopoulos, A.W.J.; Bourque, J.R.; McClain Counts, J.; Cormier, N.; Krauss, K. Stable isotope, faunal and environmental data collected from 2015 for hydrological mangrove restoration work in southwest Florida. *U.S. Geol. Surv. Data Release* **2024**. [CrossRef]
42. R Development Core Team. *R: A Language an Environment for Statistical Computing*; R Foundation for Statistical Computing: Vienna, Austria, 2018.
43. Zar, J.H. *Biostatistical Analysis*, 4th ed.; Prentice Hall: Upper Saddle River, NJ, USA, 1999.
44. Clarke, K.R.; Gorley, R.N. *PRIMER v7: User Manual/Tutorial*; PRIMER-E: Plymouth, UK, 2015.
45. Anderson, M.; Gorley, R.N.; Clarke, K.R. *PERMANOVA+ for PRIMER: Guide to Software and Statistical Methods*; PRIMER-E Ltd.: Plymouth, UK, 2008.
46. Reid, W.D.K.; Sweeting, C.J.; Wigham, B.D.; McGill, R.A.R.; Polunin, N.V.C. Isotopic niche variability in macroconsumers of the East Scotia Ridge (Southern Ocean) hydrothermal vents: What more can we learn from an ellipse? *Mar. Ecol. Prog. Ser.* **2016**, *542*, 13–24. [CrossRef]
47. Zhang, K.; Thapa, B.; Ross, M.; Gann, D. Remote sensing of seasonal changes and disturbances in mangrove forest: A case study from South Florida. *Ecosphere* **2016**, *7*, e01366. [CrossRef]
48. Murphy, A.E.; Cintra-Buenrostro, C.E.; Fierro-Cabo, A. Identifying nitrogen source and seasonal variation in a Black Mangrove (*Avicennia germinans*) community of the south Texas coast. *Aquat. Bot.* **2021**, *169*, 103339. [CrossRef]
49. Jiménez, J.A.; Lugo, A.E.; Cintrón, G. Tree Mortality in Mangrove Forests. *Biotropica* **1985**, *17*, 177–185. [CrossRef]
50. McKee, K.L.; Faulkner, P.L. Restoration of biogeochemical function in mangrove forests. *Restor. Ecol.* **2000**, *8*, 247–259. [CrossRef]
51. Knight, J.M.; Griffin, L.; Dale, P.E.R.; Sheaves, M. Short-term dissolved oxygen patterns in sub-tropical mangroves. *Estuar. Coast. Shelf Sci.* **2013**, *131*, 290–296. [CrossRef]
52. Goecke, S.D.; Carstenn, S.M. Fish communities and juvenile habitat associated with non-native *Rhizophora mangle* L. in Hawai'i. *Hydrobiologia* **2017**, *803*, 209–224. [CrossRef]
53. Sabeel, R.A.O.; Ingels, J.; Pape, E.; Vanreusel, A. Macrofauna along the Sudanese Red Sea coast: Potential effect of mangrove clearance on community and trophic structure. *Mar. Ecol.* **2014**, *36*, 794–809. [CrossRef]
54. Granek, E.; Ruttenberg, B.I. Changes in biotic and abiotic processes following mangrove clearing. *Estuar. Coast. Shelf Sci.* **2008**, *80*, 555–562. [CrossRef]
55. Alfaro, A.C. Effects of mangrove removal on benthic communities and sediment characteristics at Mangawhai Harbour, northern New Zealand. *ICES J. Mar. Sci.* **2010**, *67*, 1087–1104. [CrossRef]
56. Milbrandt, E.C.; Tinsley, M.N. The role of saltwort (*Batis maritima* L.) in regeneration of degraded mangrove forests. *Hydrobiologia* **2006**, *568*, 369–377. [CrossRef]
57. Pearson, T.R.; Rosenberg, R. Macrobenthic succession in relation to organic enrichment and pollution in the marine environment. *Oceanog. Mar. Biol. Annu. Rev.* **1978**, *16*, 229–311.
58. Linley, J.R. Biting midges of mangrove swamps and saltmarshes (Diptera: Ceratopogonidae). In *Marine Insects*; North-Holland Publishing Co.: Amsterdam, The Netherlands, 1976; pp. 335–376.
59. Glasby, C.J.; Erséus, C.; Martin, P. Annelids in extreme aquatic environments: Diversity, adaptations and evolution. *Diversity* **2021**, *13*, 98. [CrossRef]
60. Vineetha, S.; Bijoy Nandan, S.; Rakhi Gopalan, K.P. Comparative study on macrobenthic community structure with special reference to oligochaetes during drought and flooded phases in a tropical Kole Wetland, India. *Int. J. Mar. Sci.* **2015**, *5*, 1–10.
61. Pearson, S.G.; Verney, R.; van Prooijen, B.C.; Tran, D.; Hendriks, E.C.M.; Jacquet, M.; Wang, Z.B. Characterizing the composition of sand and mud suspensions in coastal and estuarine environments using combined optical and acoustic measurements. *JGR Ocean.* **2021**, *126*, e2021JC017354. [CrossRef]
62. Kristensen, E.; Bouillon, S.; Dittmar, T.; Marchand, C. Organic carbon dynamics in mangrove ecosystems: A review. *Aquat. Bot.* **2008**, *89*, 201–219. [CrossRef]
63. Kristensen, E. Mangrove crabs as ecosystem engineers; with emphasis on sediment processes. *J. Sea Res.* **2008**, *59*, 30–43. [CrossRef]
64. González-Ortiz, V.; Egea, L.G.; Jiménez-Ramos, R.; Moreno-Marín, F.; Pérez-Lloréns, J.L.; Bouma, T.; Brun, F. Submerged vegetation complexity modifies benthic infauna communities: The hidden role of the belowground system. *Mar. Ecol.* **2016**, *37*, 543–552. [CrossRef]
65. Pogado, F.O.; De Chavez, E.R.C. Diversity and community assembly patterns of gastropods in island and fringing mangrove forests in Calatagan, Batangas, Philippines. *J. Wetl. Biodivers.* **2022**, *12*, 7–23.
66. Nurfitriani, S.; Lili, W.; Hamdani, H.; Sahidin, A. Density effect of mangrove vegetation on gastropods on Pandansari mangrove ecotourism forest, Kaliwlingi Village, Brebes Central Java. *World Sci. News* **2019**, *133*, 98–120.

67. Zamprogno, G.C.; Tognella, M.M.P.; Costa, M.B.d.; Otegui, M.B.P.; Menezes, K.M. Spatio-temporal distribution of benthic fauna in mangrove areas in the Bay of Vitória estuary, Brazil. *Reg. Stud. Mar. Sci.* **2023**, *62*, 102939. [CrossRef]
68. De Haas, E.M.; Wagner, C.; Koelmans, A.A.; Michiel, H.S.K.; Admiraal, W. Habitat selection by chironomid larvae: Fast growth requires fast food. *J. Anim. Ecol.* **2006**, *75*, 148–155. [CrossRef]
69. Panatta, Á.; Stenert, C.; Martins dos Santos, E.; Maltchik, L. Diversity and distribution of chironomid larvae in wetlands in Southern Brazil. *J. Kans. Entomol. Soc.* **2007**, *80*, 229–242.
70. Whitcraft, C.R.; Levin, L.A. Regulation of benthic algal and animal communities by salt marsh plants: Impact of shading. *Ecology* **2007**, *88*, 904–917. [CrossRef]
71. Currin, C.A.; Newell, S.Y.; Paerl, H.W. The role of standing dead Spartina alterniflora and benthic microalgae in salt marsh food webs: Considerations based on multiple stable isotope analysis. *Mar. Ecol. Prog. Ser.* **1995**, *121*, 99–116. [CrossRef]
72. Alfaro, A.C. Diet of *Littoraria scabra*, while vertically migrating on mangrove trees: Gut content, fatty acid, and stable isotope analyses. *Estuar. Coast. Shelf Sci.* **2008**, *79*, 718–726. [CrossRef]
73. Nordström, M.C.; Currin, C.A.; Talley, T.S.; Whitcraft, C.R.; Levin, L.A. Benthic food-web succession in a developing salt marsh. *Mar. Ecol. Prog. Ser.* **2014**, *500*, 43–55. [CrossRef]